The structure of the proton from numerical simulations of lattice QCD

Martha Constantinou



Temple University

High Energy Theory - RIKEN seminar

October 13, 2022

Collaborators

Twist-2 PDFs and GPDs

- **C. Alexandrou**
  Univ. of Cyprus/Cyprus Institute
- **K. Cichy**
  Adam Mickiewicz University
- **J. Delmar**
  Temple University
- **K. Hadjiyiannakou**
  Cyprus Institute
- **K. Jansen**
  DESY, Zeuthen
- **F. Manigrasso**
  Univ. of Cyprus
- **A. Scapellato**
  Temple University
- **F. Steffens**
  University of Bonn



ETMC Meeting 2008

Twist-3 PDFs and GPDs

- **S. Bhattacharya**
  Brookhaven National Lab
- **K. Cichy**
  Adam Mickiewicz University
- **J. Dodson**
  Temple University
- **A. Metz**
  Temple University
- **A. Scapellato**
  Temple University
- **F. Steffens**
  University of Bonn



TMD Meeting 2016

Novel approach on GPDs

- **S. Bhattacharya**
  Brookhaven National Lab
- **K. Cichy**
  Adam Mickiewicz University
- **J. Dodson**
  Temple University
- **X. Gao**
  Argonne National Lab
- **A. Metz**
  Temple University
- **S. Mukherjee**
  Brookhaven National Lab
- **F. Steffens**
  University of Bonn
- **Y. Zhao**
  Argonne National Lab



In the quest of solving complex problems

$$\mathscr{L}_{\mathrm{QCD}} = \sum_f \bar{\psi}_f \left(i\gamma^\mu D_\mu - m_f \right) \psi_f - \frac{1}{4} F^a_{\mu\nu} F^{a\,\mu\nu}$$

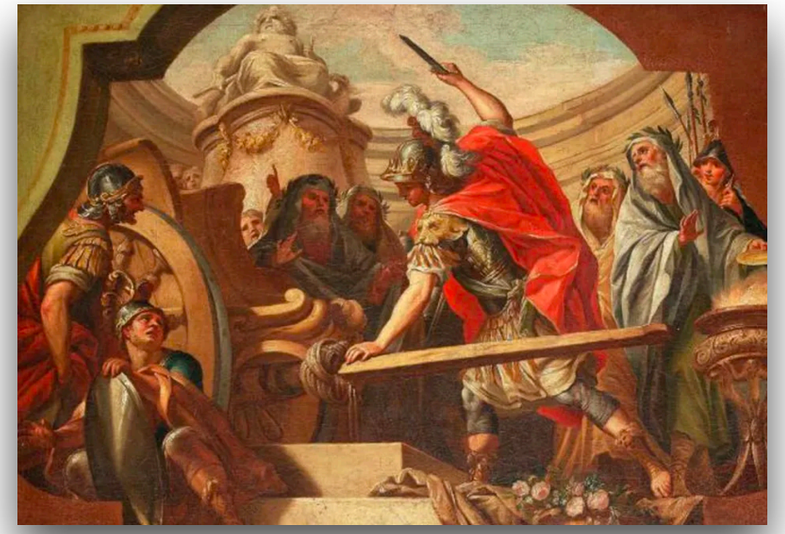
"Simulate non-analytical systems"





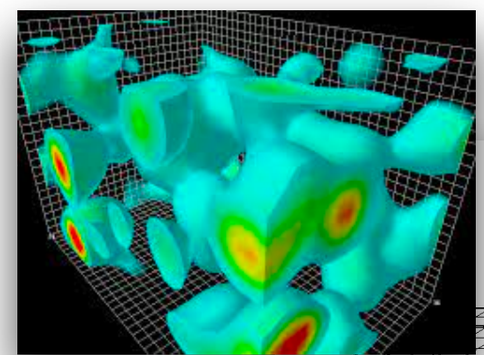


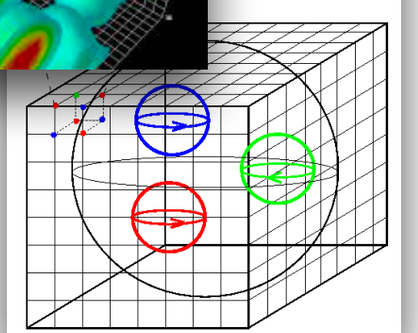




"Οτι δεν λύνεται, κόβεται"

Alexander the Great while cutting the Gordian knot

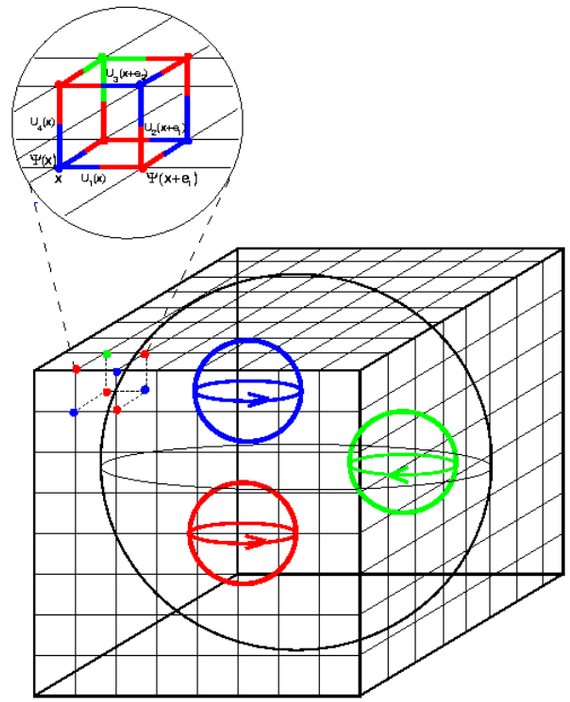




Hot & Cold QCD and beyond

Lattice formulation of QCD

Ideal first principle formulation of QCD
(simulations starting from original Lagrangian)



★ Space-time discretization on a finite-size 4-D lattice

★ Serves as a regulator:
UV cut-off: inverse lattice spacing $\int_{-\infty}^{\infty} dp \rightarrow \int_{-\pi/a}^{\pi/a} \frac{dp}{2\pi}$

IR cut-off: inverse lattice size $\int dpF(p) \rightarrow \sum_{n}^{N_{\max}} \frac{2\pi}{L} F(p_0 + \frac{2\pi n}{L})$

★ Removal of regulator $L \rightarrow \infty\,, \quad a \rightarrow 0$

Technical Aspects

★ Parameters (define cost of simulations):
quark masses (aim at physical values)
lattice spacing (ideally fine lattices)
lattice size (need large volumes)

★ Discretization not unique:
Wilson, Clover, Twisted Mass, Staggered, Overlap, Domain Wall, Mixed actions

USQCD Nuclear Physics Program

★ Important lattice QCD contributions that complement the experimental program of major facilities



★ BNL is supporting lattice QCD activities through their computational center

Hadrons from their partonic structure

★ Quarks and gluons are fundamental degrees of freedom in QCD

★ Structure of hadrons explored in high-energy scattering processes

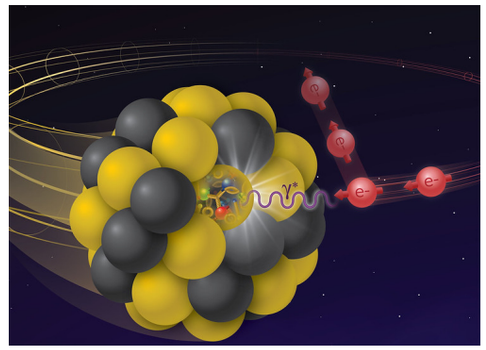
★ Due to asymptotic freedom, e.g.

$$\sigma_{\rm DIS}(x,Q^2) = \sum_i \left[H^i_{\rm DIS} \otimes f_i\right](x,Q^2)$$

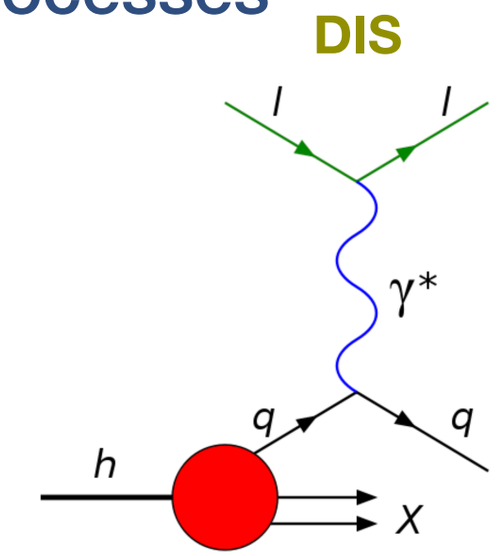
$$[a\otimes b](x) \equiv \int_x^1 \frac{d\xi}{\xi}\, a\left(\frac{x}{\xi}\right) b(\xi)$$

Perturb. part (process dependent)

Non-Perturb. part (process "independent")

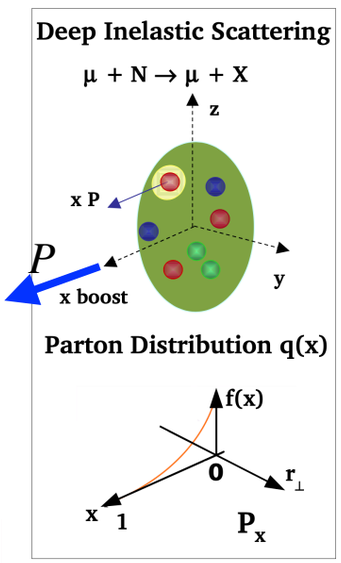


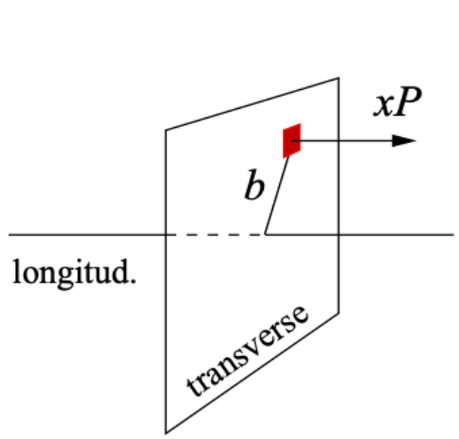
Collisions @ EIC

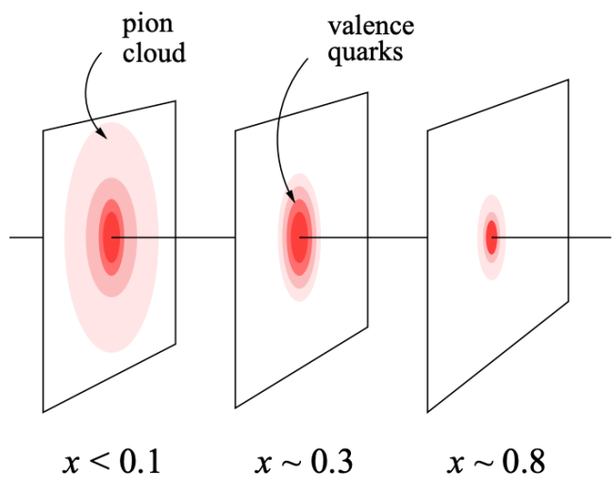


Accessed in lattice QCD through appropriate operators

★ f_i provides information on partonic structure







tomographic images of quark distribution in nucleon at fixed longitudinal momentum

[H. Abramowicz et al., whitepaper for NSAC LRP, 2007]

Twist-classification of PDFs, GPDs, TMDs

$$f_i = f_i^{(0)} + \frac{f_i^{(1)}}{Q} + \frac{f_i^{(2)}}{Q^2} \cdots$$

Twist-2 $(f_i^{(0)})$

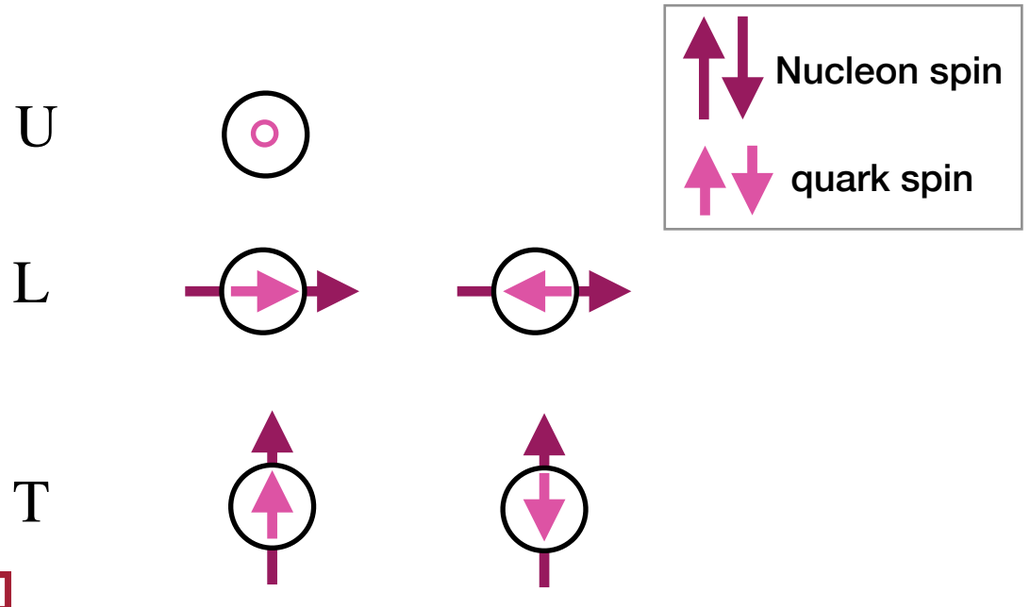
Nucleon \ Quark	U (γ^+)	L ($\gamma^+\gamma^5$)	T (σ^{+j})
U	$H(x,\xi,t)$ $E(x,\xi,t)$ unpolarized		
L		$\widetilde{H}(x,\xi,t)$ $\widetilde{E}(x,\xi,t)$ helicity	
T			H_T, E_T $\widetilde{H}_T, \widetilde{E}_T$ transversity

Twist-3 $(f_i^{(1)})$

Nucleon \ $\mathcal{O}$	γ^j	$\gamma^j\gamma^5$	σ^{jk}
U	G_1, G_2 G_3, G_4		
L		$\widetilde{G}_1, \widetilde{G}_2$ $\widetilde{G}_3, \widetilde{G}_4$	
T			$H_2'(x,\xi,t)$ $E_2'(x,\xi,t)$

Selected

Probabilistic interpretation



- ★ Lack density interpretation, but can be sizable
- ★ Kinematically suppressed
  Difficult to isolate experimentally
- ★ Theoretically: contain $\delta(x)$ singularities
- ★ Contain info on quark-gluon-quark correlators

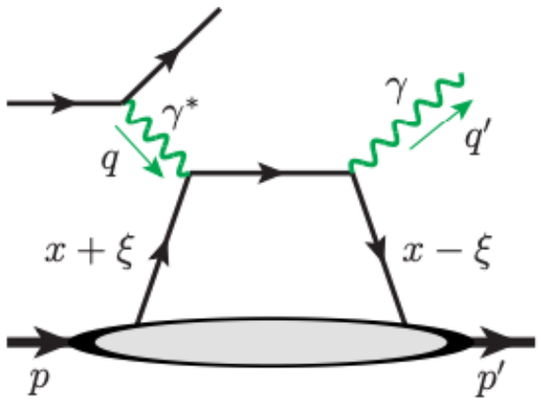
Generalized Parton Distributions

★ Crucial in understanding hadron tomography

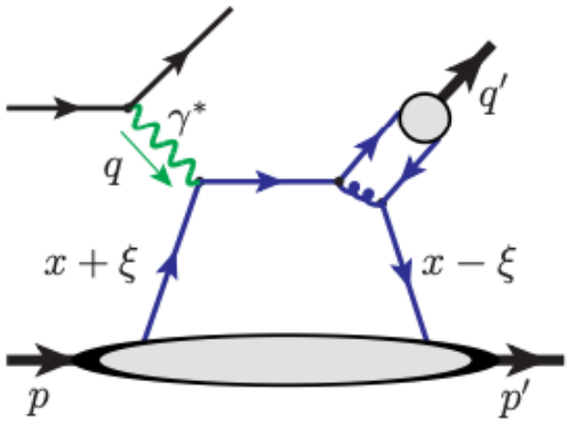
★ GPDs may be accessed via exclusive reactions (DVCS, DVMP)

[X.-D. Ji, PRD 55, 7114 (1997)]

DVCS

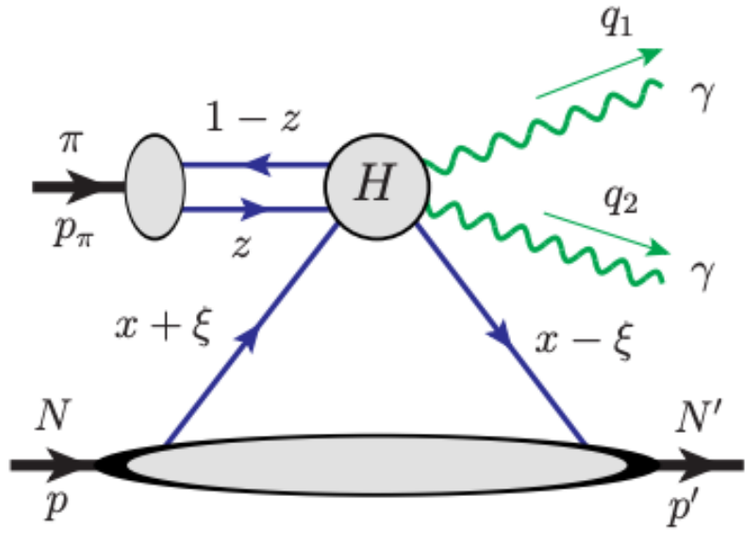


DVMP



★ exclusive pion-nucleon diffractive production of a γ pair of high $p_\perp$

[J. Qiu et al, arXiv:2205.07846]



Generalized Parton Distributions

★ GPDs are not well-constrained experimentally:

- x-dependence extraction is not direct. DVCS amplitude: $\mathscr{H} = \int_{-1}^{+1} \frac{H(x,\xi,t)}{x-\xi+i\epsilon} dx$

  (SDHEP [J. Qiu et al, arXiv:2205.07846] gives access to x)

- independent measurements to disentangle GPDs

- GPDs phenomenology more complicated than PDFs (multi-dimensionality)

- and more challenges …

★ Essential to complement the knowledge on GPD from lattice QCD

★ Lattice data may be incorporated in global analysis of experimental data and may influence parametrization of t and ξ dependence

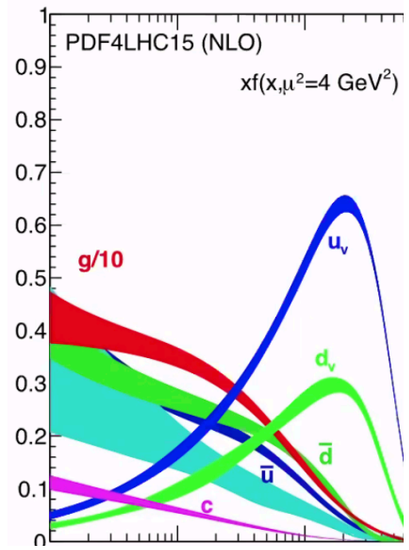
Generalized Parton Distributions

★ **PDFs, GPDs, TMDs parameterized in terms of off-forward matrix elements of non-local light-cone operators (Not accessible on Euclidean lattice)**

[R. P. Feynman, Phys. Rev. Lett. 23, 1415 (1969)]

$$F_\Gamma(x,\xi,q^2) = \frac{1}{2}\int \frac{d\lambda}{2\pi} e^{ix\lambda} \langle p'|\bar{\psi}(-\lambda n/2)\,\mathcal{O}\,\underbrace{\mathcal{P}e^{ig\int_{-\lambda/2}^{\lambda/2} d\alpha n\cdot A(n\alpha)}}_{\text{gauge invariance}}\psi(\lambda n/2)|p\rangle$$

$q = p' - p$, $\bar{P} = (p'+p)/2$, n: **light-cone vector** ($\bar{P}.n = 1$), $\xi = -n\cdot\Delta/2$

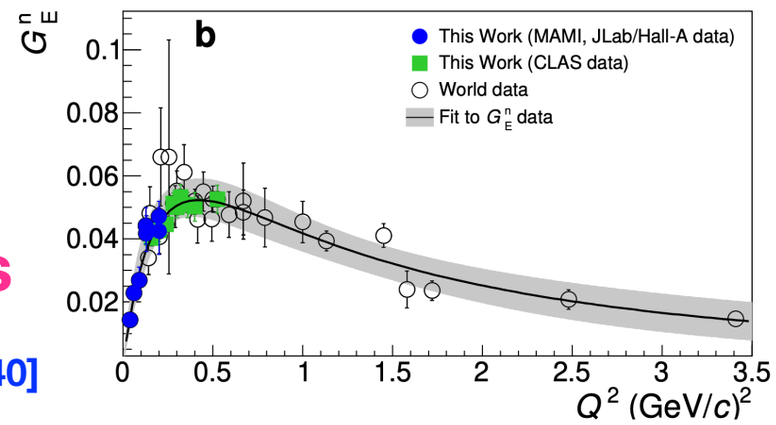


★ **Their Mellin moments with respect to x can be accessed in LQCD, e.g.,**

$$\langle x^{n-1}\rangle = \int_{-1}^{+1} x^{n-1} f(x)\,dx$$

★ **Mellin moments of GPDs:**
Form factors & generalized form factors

[H. Atac, Nature Commun. 12 (2021) 1, 1759, arXiv:2103.10840]



Accessing information on GPDs

★ **Mellin moments**
(local OPE expansion)

$$\bar{q}(-\tfrac{1}{2}z)\,\gamma^\sigma W[-\tfrac{1}{2}z,\tfrac{1}{2}z]\,q(\tfrac{1}{2}z) \;=\; \sum_{n=0}^{\infty}\frac{1}{n!}\,z_{\alpha_1}\dots z_{\alpha_n}\Big[\bar{q}\gamma^\sigma \overleftrightarrow{D}^{\alpha_1}\dots\overleftrightarrow{D}^{\alpha_n} q\Big]$$

local operators

$$\langle N(P')|\mathcal{O}_V^{\mu\mu_1\cdots\mu_{n-1}}|N(P)\rangle \sim \sum_{\substack{i=0\\ \text{even}}}^{n-1}\left\{\gamma^{\{\mu}\Delta^{\mu_1}\cdots\Delta^{\mu_i}\overline{P}^{\mu_{i+1}}\cdots\overline{P}^{\mu_{n-1}\}}A_{n,i}(t) - i\frac{\Delta_\alpha\sigma^{\alpha\{\mu}}}{2m_N}\Delta^{\mu_1}\cdots\Delta^{\mu_i}\overline{P}^{\mu_{i+1}}\cdots\overline{P}^{\mu_{n-1}\}}B_{n,i}(t)\right\} + \frac{\Delta^\mu\Delta^{\mu_1}\cdots\Delta^{\mu_{n-1}}}{m_N}C_{n,0}(\Delta^2)\Big|_{n\ \text{even}}\Big)\Big\}$$

★ **Matrix elements of non-local operators**
(quasi-GPDs, pseudo-GPDs, …)

$$\langle N(P_f)\,|\,\bar{\Psi}(z)\,\Gamma\,\mathscr{W}(z,0)\Psi(0)\,|\,N(P_i)\rangle_\mu$$

Wilson line

$$\langle N(P')|O_V^\mu(x)|N(P)\rangle = \overline{U}(P')\left\{\gamma^\mu H(x,\xi,t) + \frac{i\sigma^{\mu\nu}\Delta_\nu}{2m_N}E(x,\xi,t)\right\}U(P) + \text{ht}\,,$$

$$\langle N(P')|O_A^\mu(x)|N(P)\rangle = \overline{U}(P')\left\{\gamma^\mu\gamma_5\widetilde{H}(x,\xi,t) + \frac{\gamma_5\Delta^\mu}{2m_N}\widetilde{E}(x,\xi,t)\right\}U(P) + \text{ht}\,,$$

$$\langle N(P')|O_T^{\mu\nu}(x)|N(P)\rangle = \overline{U}(P')\left\{i\sigma^{\mu\nu}H_T(x,\xi,t) + \frac{\gamma^{[\mu}\Delta^{\nu]}}{2m_N}E_T(x,\xi,t) + \frac{\overline{P}^{[\mu}\Delta^{\nu]}}{m_N^2}\widetilde{H}_T(x,\xi,t) + \frac{\gamma^{[\mu}\overline{P}^{\nu]}}{m_N}\widetilde{E}_T(x,\xi,t)\right\}U(P) + \text{ht}$$

Mellin moments of PDFs and GPDs

★ Advantages

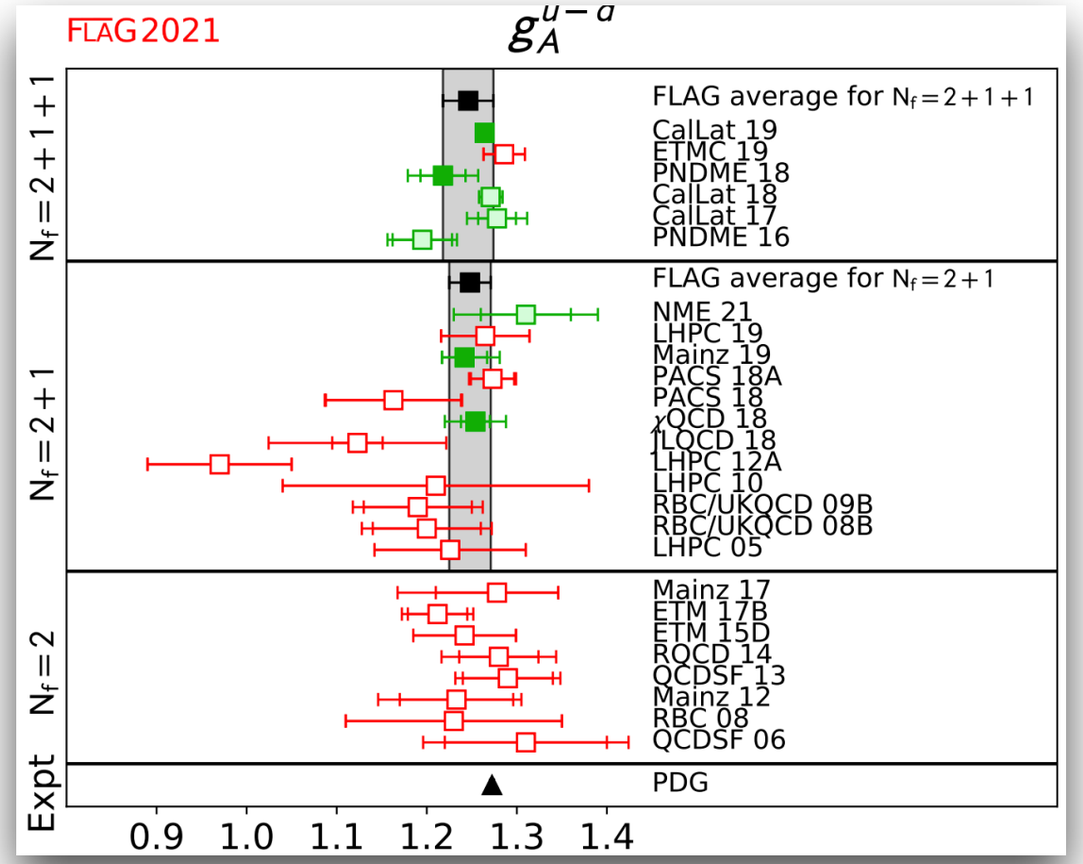
- Frame independence
- Several values of momentum transfer with same computational cost
- Form factors extracted with controlled statistical uncertainties

★ Disadvantages

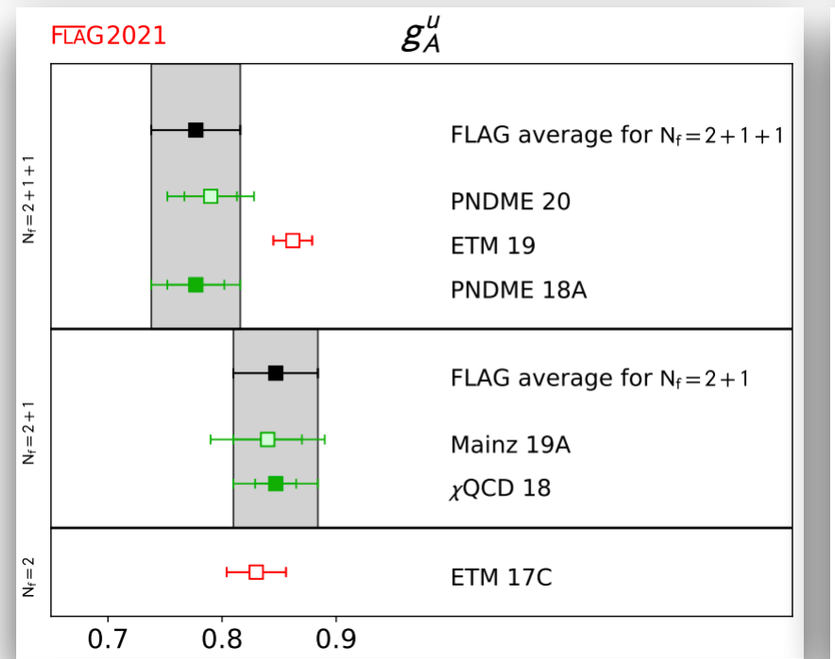
- x dependence is integrated out
- GFFs are skewness independence
- Geometrical twist classification (coincides with dynamical twist of scattering processes only at leading order)
- Signal-to-noise ratio decays with the addition of covariant derivatives
- Power-divergent mixing for high Mellin moments (derivatives > 3)
- Number of GFFs increases with order of Mellin moment

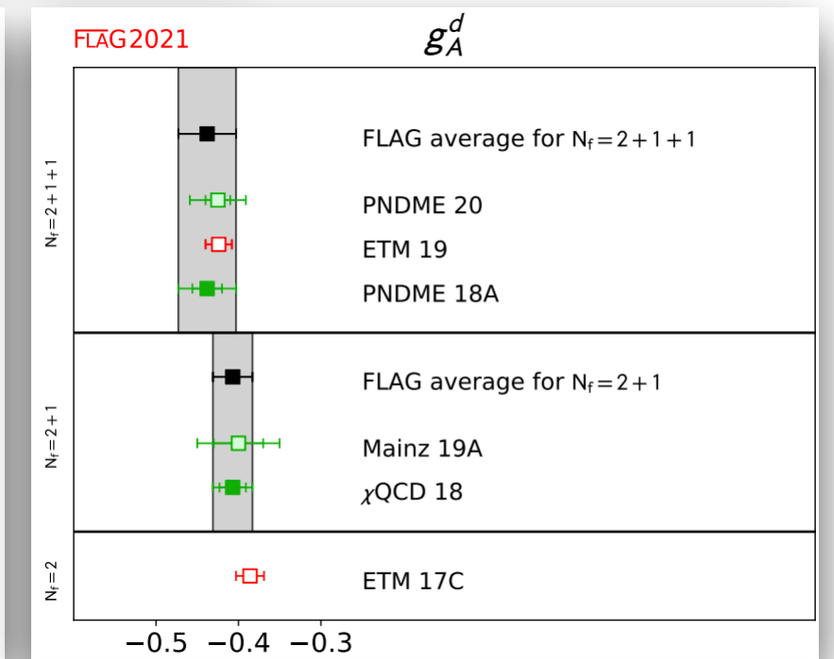
$$\langle N(P')|\mathcal{O}_V^{\mu\mu_1\cdots\mu_{n-1}}|N(P)\rangle = \overline{U}(P')\left[\sum_{\substack{i=0\\ \text{even}}}^{n-1}\left\{\gamma^{\{\mu}\Delta^{\mu_1}\cdots\Delta^{\mu_i}\overline{P}^{\mu_{i+1}}\cdots\overline{P}^{\mu_{n-1}\}}A_{n,i}(t) - i\frac{\Delta_\alpha\sigma^{\alpha\{\mu}}{2m_N}\Delta^{\mu_1}\cdots\Delta^{\mu_i}\overline{P}^{\mu_{i+1}}\cdots\overline{P}^{\mu_{n-1}\}}B_{n,i}(t)\right\} + \frac{\Delta^\mu\Delta^{\mu_1}\cdots\Delta^{\mu_{n-1}}}{m_N}C_{n,0}(\Delta^2)\Big|_{n\text{ even}}\right]U(P)$$

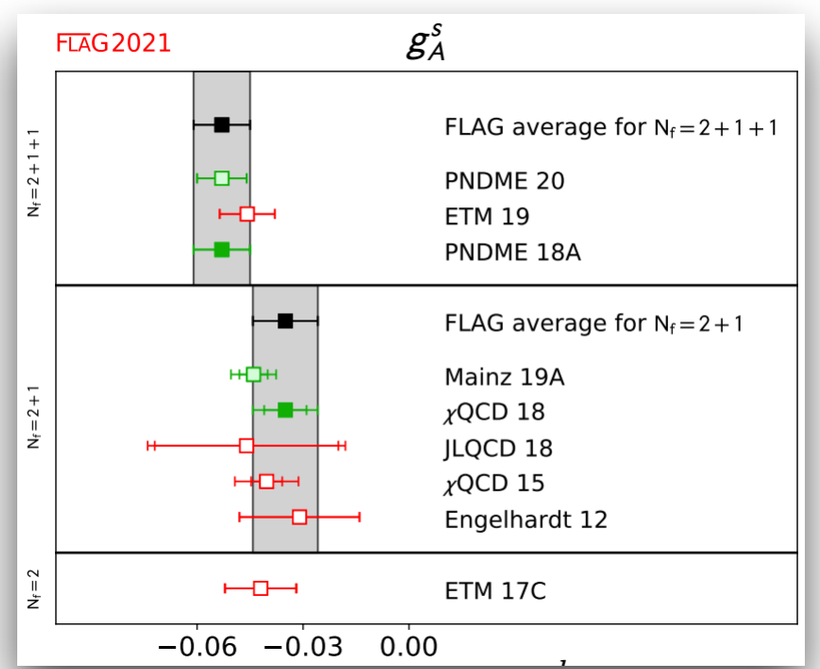
Nucleon charges



- Charges are the most well studied quantities by several groups
- Control of systematic uncertainties has already been achieved in some studies
- Flavor decomposition is part of many calculations





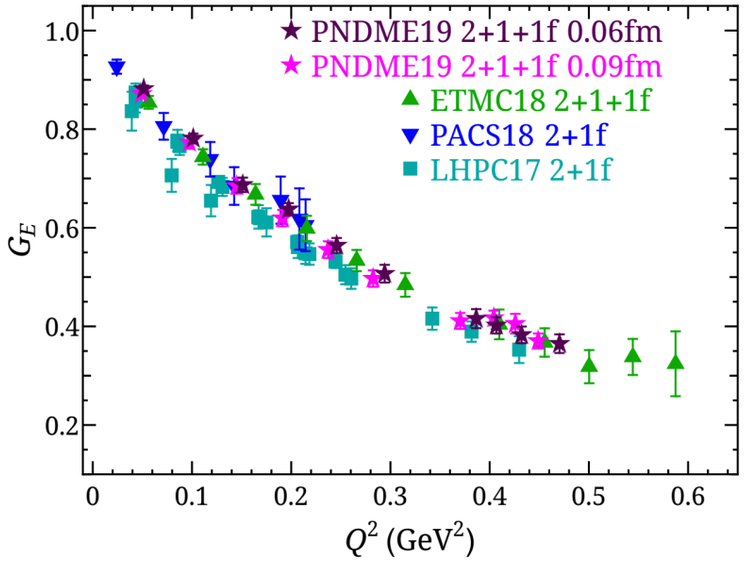


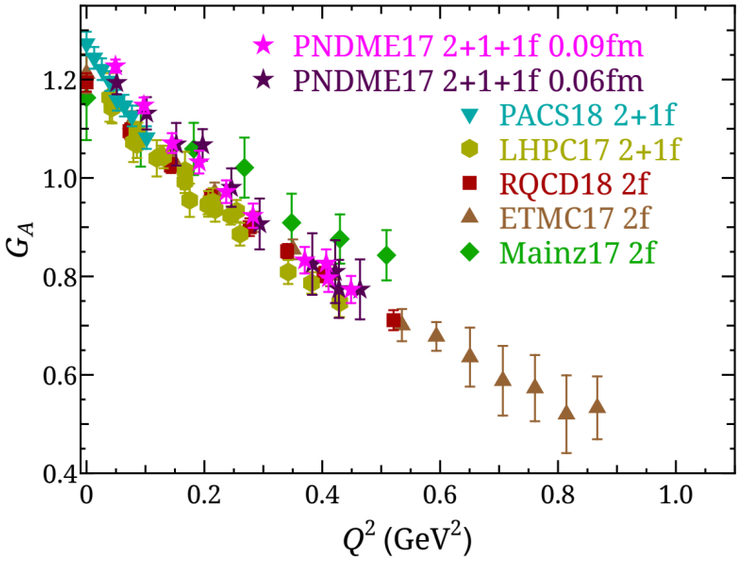
Form Factors

★ Ultra-local operators (FFS)

$$\langle N(P')|\overline{q}(0)\gamma^{\mu}q(0)|N(P)\rangle = \overline{U}(P')\left\{\gamma^{\mu}F_1(t) + \frac{i\sigma^{\mu\nu}\Delta_{\nu}}{2m_N}F_2(t)\right\}U(P)\,,$$

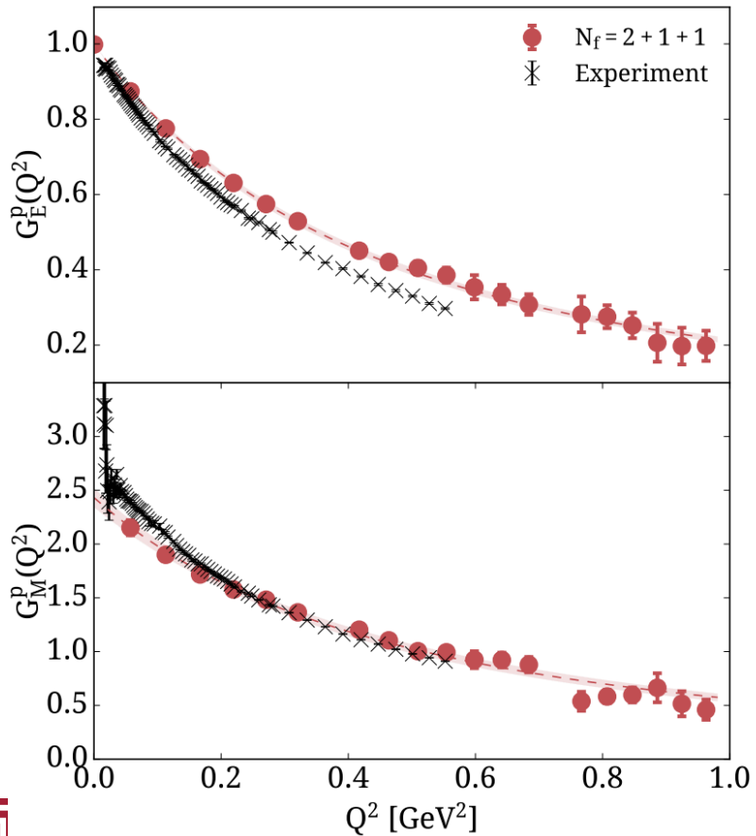
$$\langle N(P')|\overline{q}(0)\gamma^{\mu}\gamma_5 q(0)|N(P)\rangle = \overline{U}(P')\left\{\gamma^{\mu}\gamma_5 G_A(t) + \frac{\gamma_5\Delta^{\mu}}{2m_N}G_P(t)\right\}U(P)$$

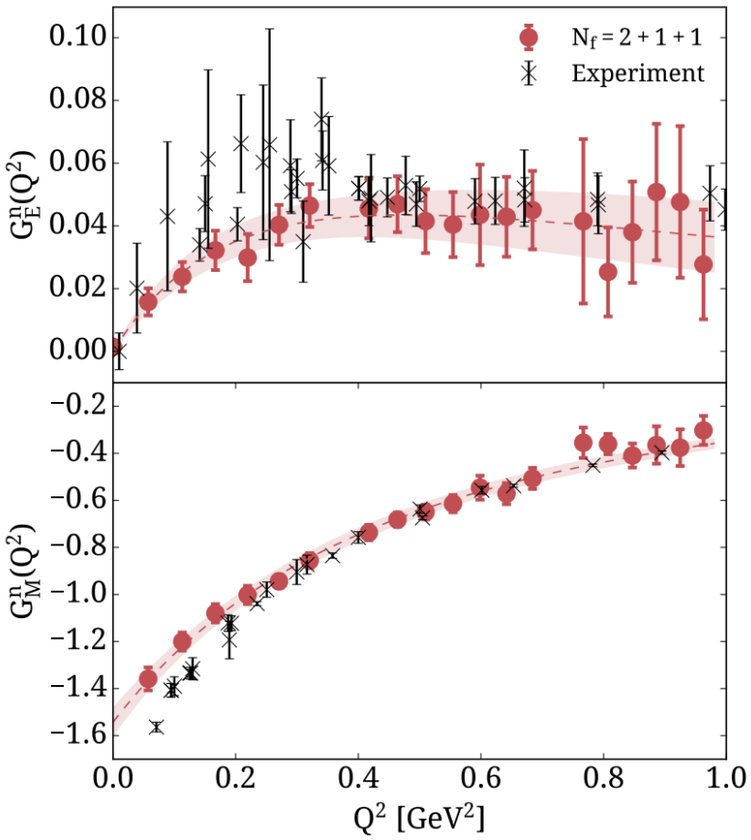




- Simulations at physical point available by multiple groups
- Precision data era
- Towards control of systematic uncertainties

[M. Constantinou et al. (2020 PDFLattice Report), Prog. Part. Nucl. Phys. 121 (2021) 103908]





- Flavor decomposition is possible
- Lattice results can complement experimental data wherever knowledge is limited

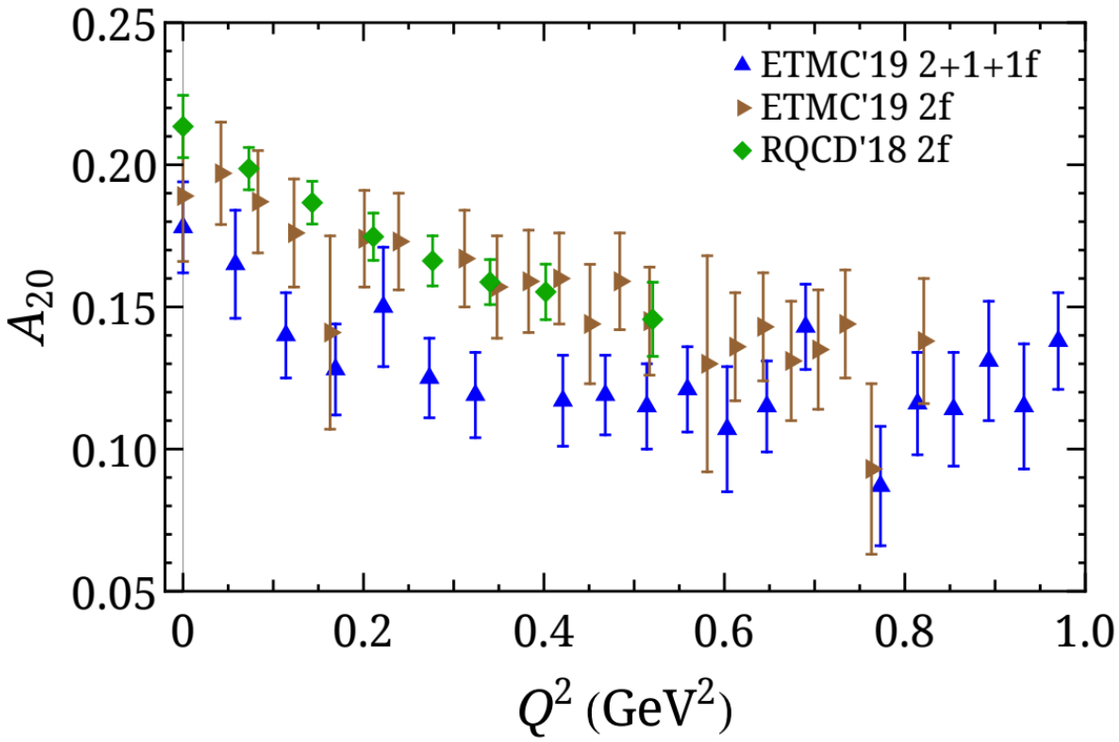
[C. Alexandrou et al., PRD 100, 014509 (2019)]

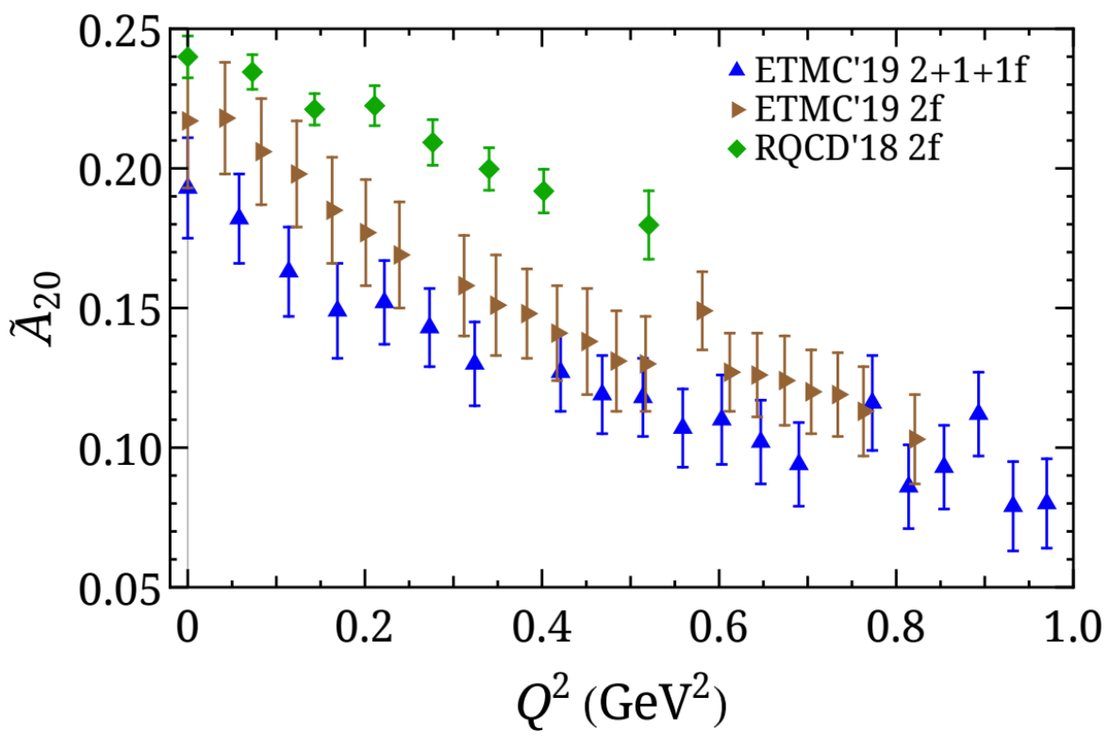
Generalized Form Factors

★ 1-derivative operators (GFFs)

$$\langle N(p',s')|\mathcal{O}_V^{\mu\nu}|N(p,s)\rangle = \bar{u}_N(p',s')\frac{1}{2}\Big[A_{20}(q^2)\,\gamma^{\{\mu}P^{\nu\}} + B_{20}(q^2)\,\frac{i\sigma^{\{\mu\alpha}q_\alpha P^{\nu\}}}{2m_N} + C_{20}(q^2)\,\frac{1}{m_N}q^{\{\mu}q^{\nu\}}\Big]u_N(p,s),$$

$$\langle N(p',s')|\mathcal{O}_A^{\mu\nu}|N(p,s)\rangle = \bar{u}_N(p',s')\frac{i}{2}\Big[\tilde{A}_{20}(q^2)\,\gamma^{\{\mu}P^{\nu\}}\gamma^5 + \tilde{B}_{20}(q^2)\,\frac{q^{\{\mu}P^{\nu\}}}{2m_N}\gamma^5\Big]u_N(p,s),$$





[M. Constantinou et al. (2020 PDFLattice Report), Prog.Part.Nucl.Phys. 121 (2021) 103908]

- Lesser studied compared to FFs at physical point
- Decay of signal-to-noise ratio

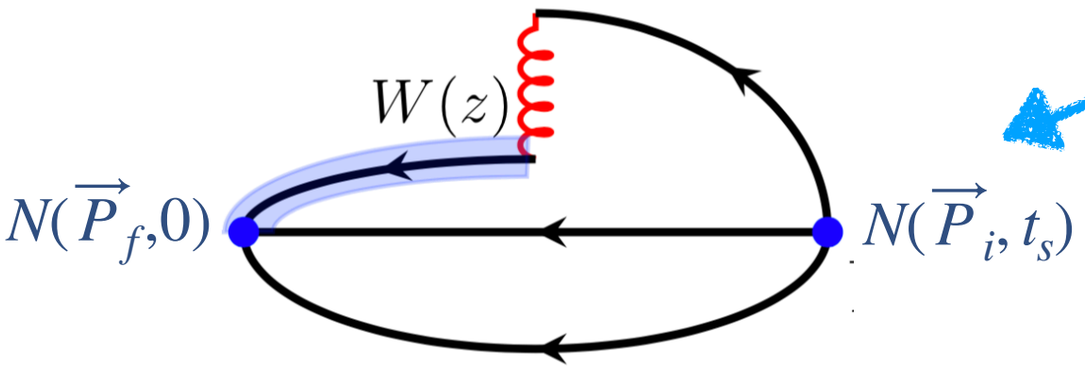
x-dependence of parton distribution

x-dependence from Euclidean lattice

[X. Ji, Phys. Rev. Lett. 110 (2013) 262002]

Matrix elements of nonlocal (equal-time) operators with boosted hadrons

$$\tilde{q}^{\mathrm{GPD}}_{\Gamma}(x,t,\xi,P_3,\mu) = \int \frac{dz}{4\pi} e^{-i\,x\,P_3\,z} \quad \langle N(P_f)\,|\,\bar{\Psi}(z)\,\Gamma\,\mathscr{W}(z,0)\Psi(0)\,|\,N(P_i)\rangle_{\mu}$$



$$\Delta = P_f - P_i$$

$$t = \Delta^2 = -Q^2$$

$$\xi = \frac{Q_3}{2P_3}$$

Variables of the calculation:

- length of the Wilson line (z)
- nucleon momentum boost (P_3)
- momentum transfer (t)
- skewness (ξ)

Such matrix elements may be analyzed through LaMET formalism (quasi—GPDs) or coordinate space factorization (pseudo-ITD)

Complementarity is important!

1. hadronic matrix elements

2. Identification of ground state

3. Renormalization

4. “form factors” disentanglement

5. x-dependence reconstruction

6. Matching to light-cone GPDs

quasi distribution approach

$$H_q(x,t,\xi,\mu_0,(\mu_0)_3,P_3) = \int_{-1}^{1} \frac{dy}{|y|} C_H\left(\frac{x}{y},\frac{\xi}{y},\frac{\mu}{yP_3},\frac{(\mu_0)_3}{yP_3},r\right) F_H(y,t,\xi,\mu) + \mathcal{O}\left(\frac{m^2}{P_3^2},\frac{t}{P_3^2},\frac{\Lambda^2_{\rm QCD}}{x^2P_3^2}\right)$$

Colinear isovector PDFs

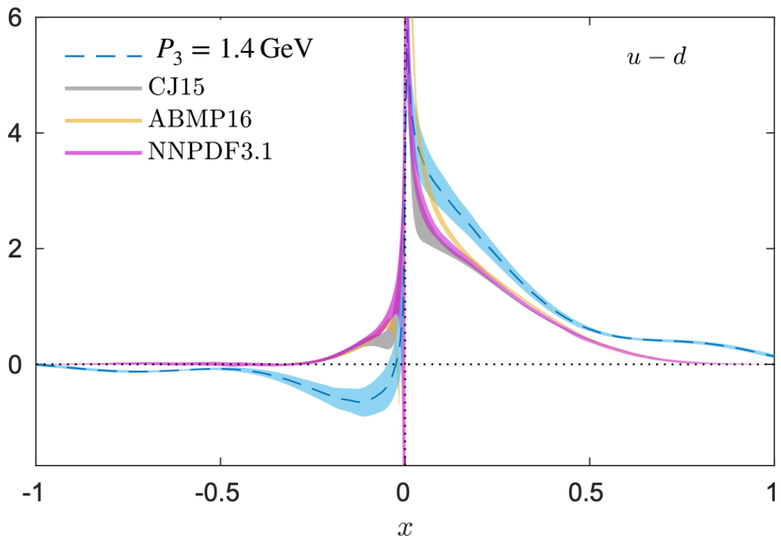
(status: toward controlling systematic uncertainties)

PDFs at physical pion mass

★ First complete study of quasi-PDFs including all steps

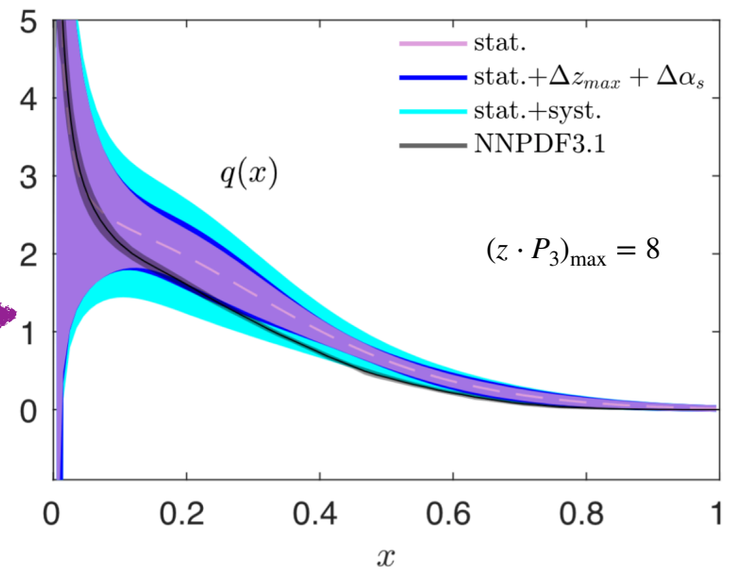
β=2.10,	$c_{\rm SW}$=1.57751, a=0.0938(3)(2) fm
$48^3 \times 96$	$a\mu = 0.0009$ $m_N = 0.932(4)$ GeV
$L = 4.5$ fm	$m_\pi = 0.1304(4)$ GeV $m_\pi L = 2.98(1)$

Quasi-PDFs

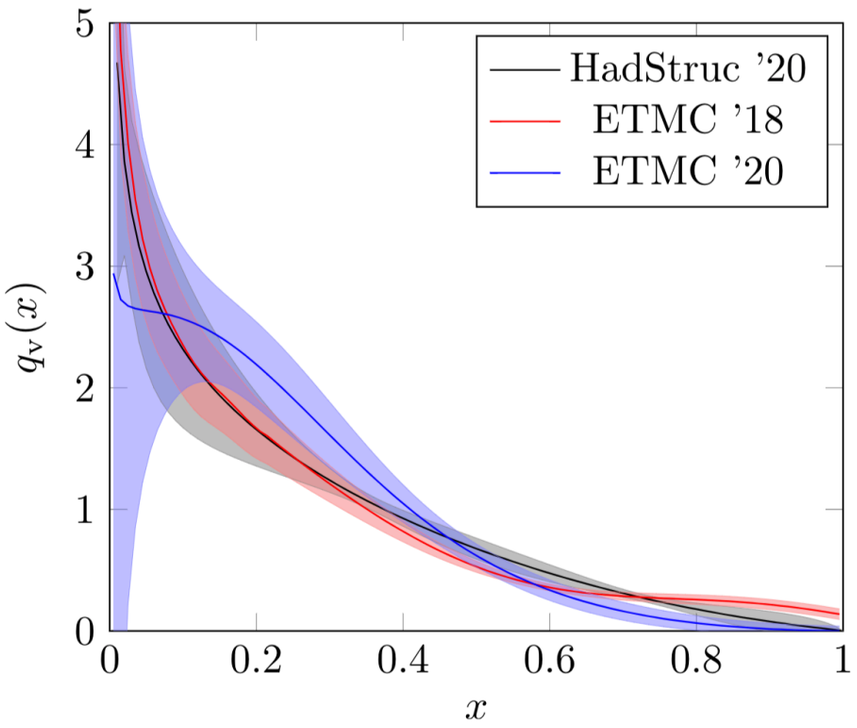


Same matrix elements

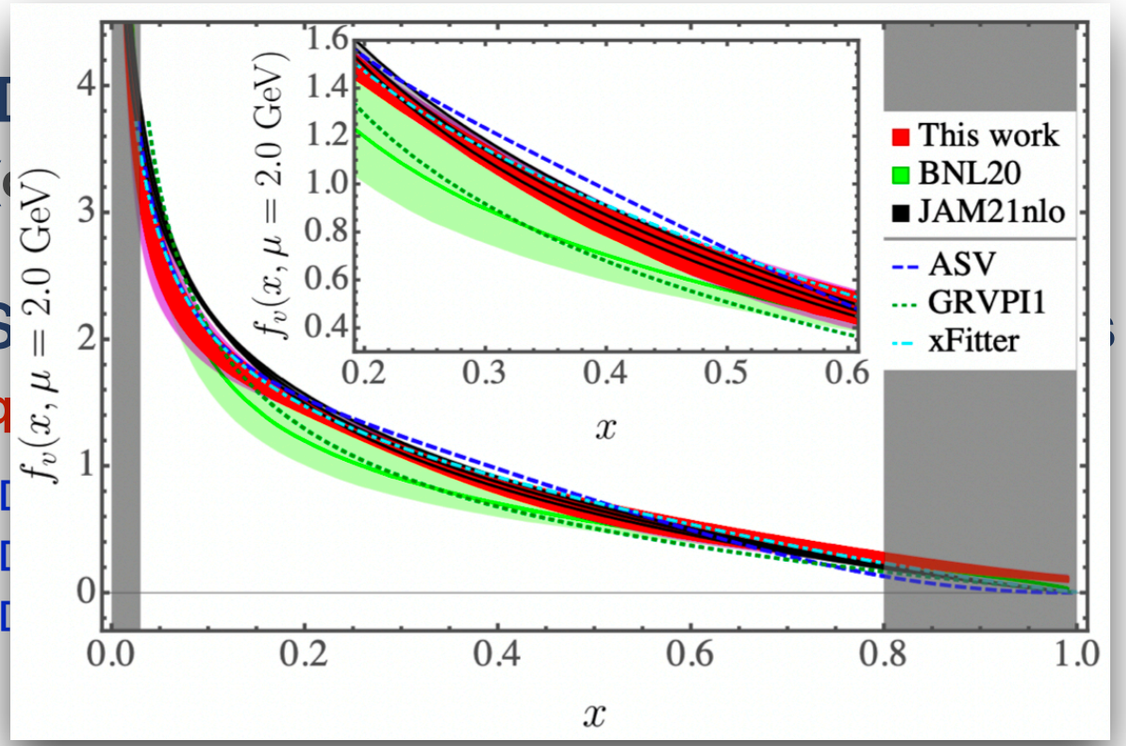
Pseudo-ITDs



[C. Alexandrou et al. (ETMC), PRL 121 (2018) 112001, arXiv:1803.02685]



[M. Bhat et al. (ETMC), arXiv:2005.02102]



[Yong Zhao et al., PRL 128, 142003 (2022)]

Flavor decomposition of PDFs

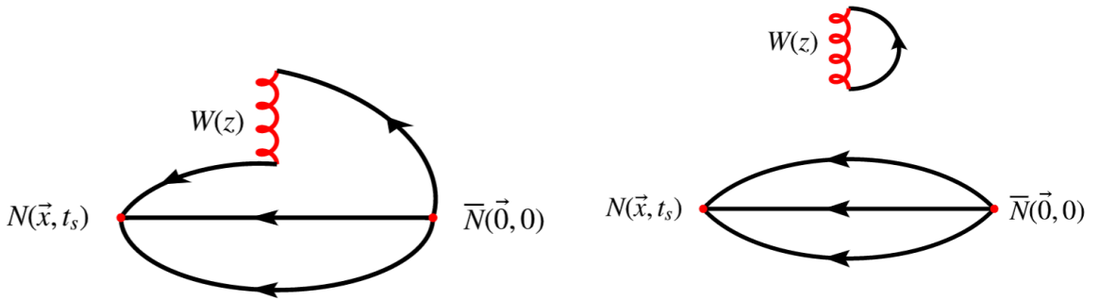
&

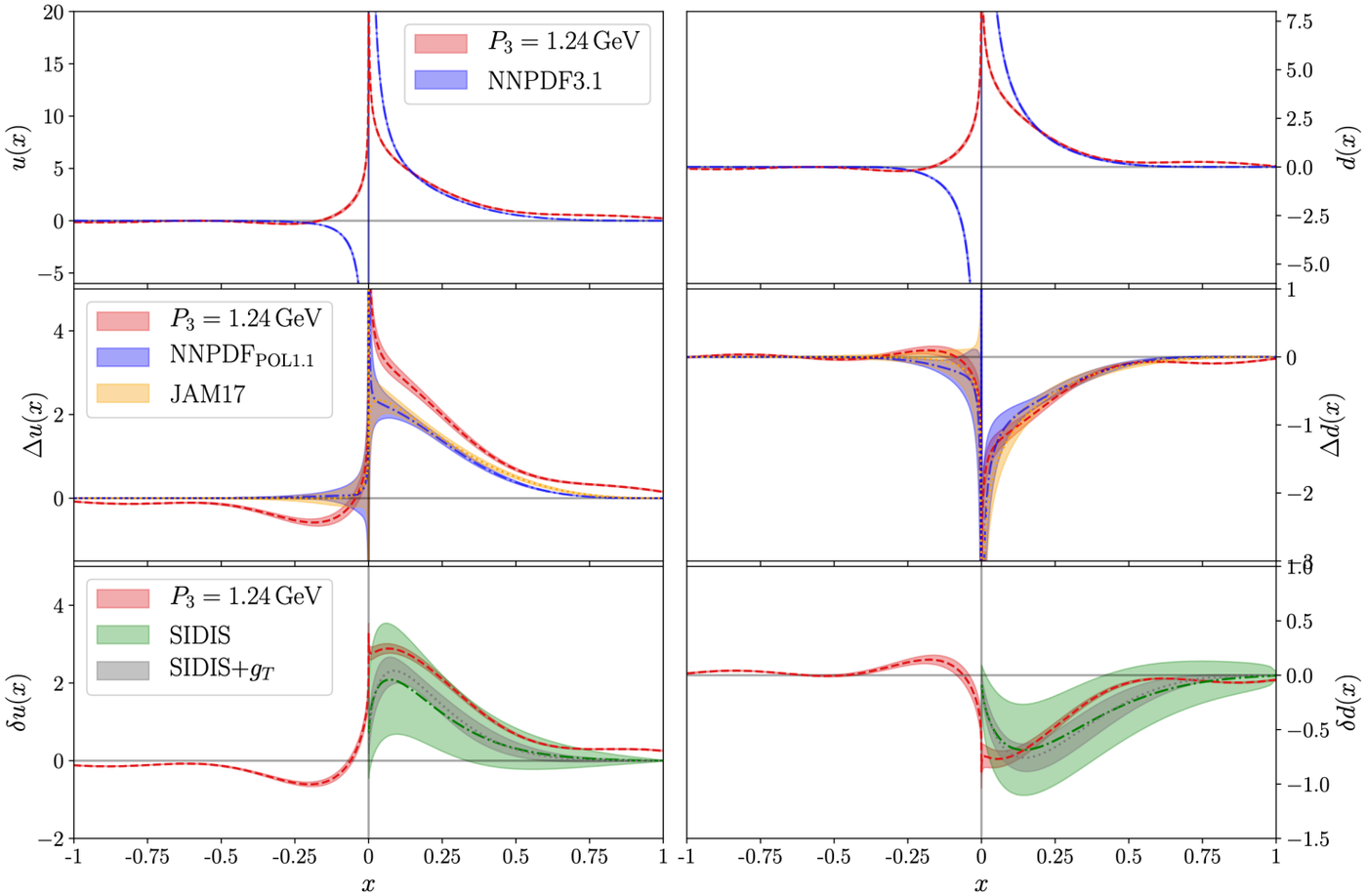
gluon PDFs

(status: taming statistical uncertainties)

Flavor decomposition of PDFs

★ **Major achievement of the field**
(due to theoretical and algorithmic developments)





$\beta = 1.726,\ c_{\mathrm{SW}} = 1.74,\ a = 0.0938(3)(2)$ fm	
$32^3 \times 64,\ L = 3.0\,\mathrm{fm}$	$a\mu_l = 0.003$ $m_\pi \approx 260\,\mathrm{MeV}$ $m_\pi L \approx 3$ $m_N = 1.09(6)$ GeV

★ **Individual-quark unpolarized, helicity, transversity PDFs**

★ **At least one order higher statistics for disconnected diagrams**

[C. Alexandrou et al., PRL 126 (2021) 10, arXiv:2009.13061; PRD 104 (2021) 5, 054503, arXiv:2106.16065]

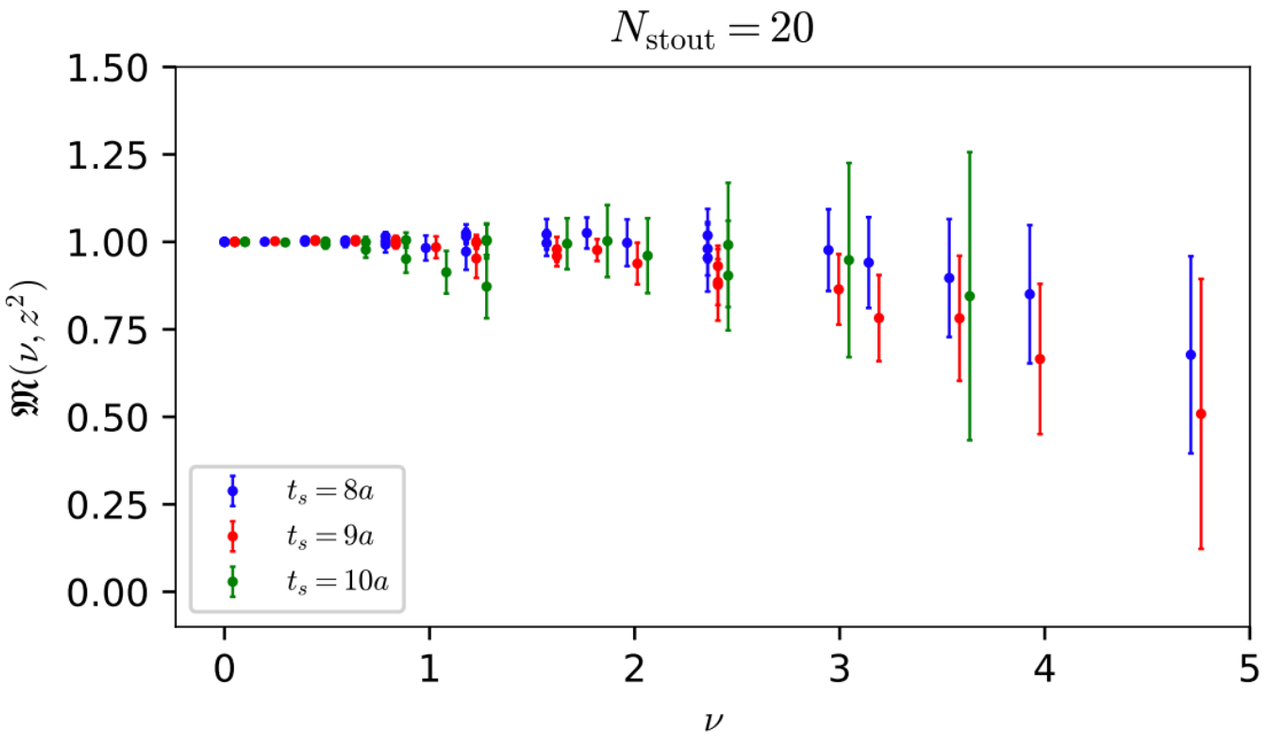
★ **Helicity PDF: most sizable disconnected light-quark contributions**

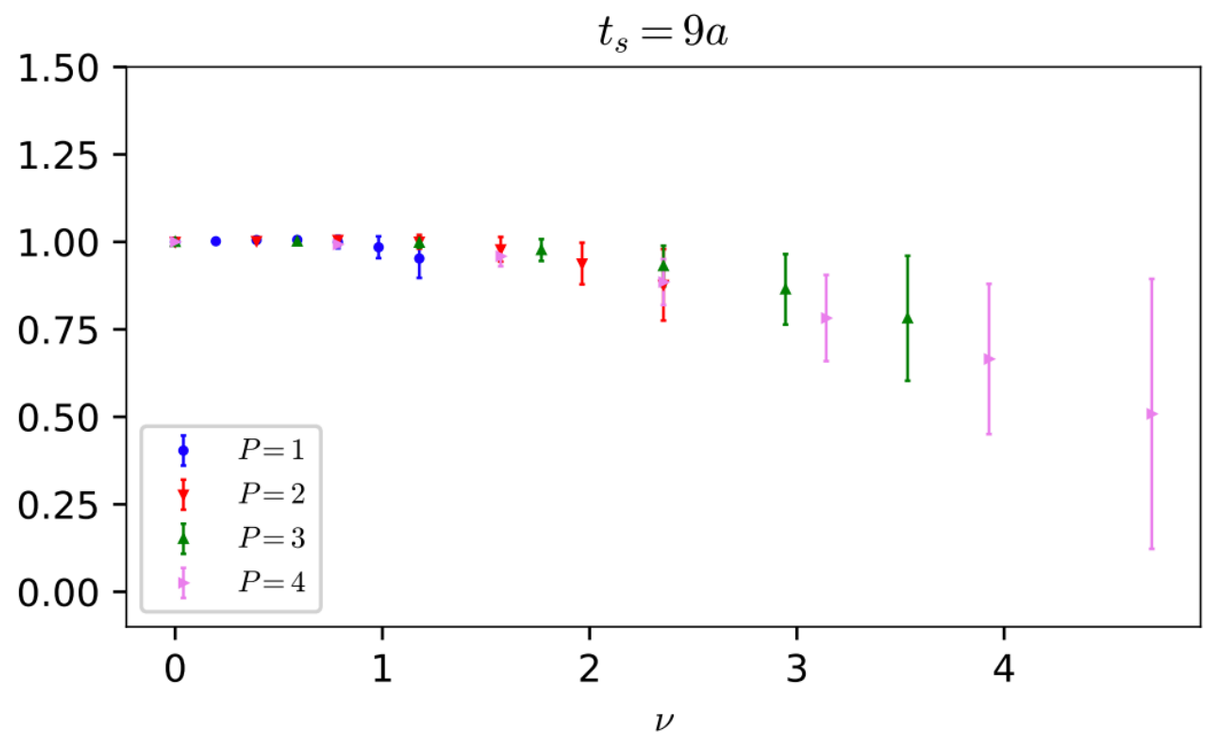
★ **Mixing with gluon PDFs to be addressed (important for s-quark PDFs)**

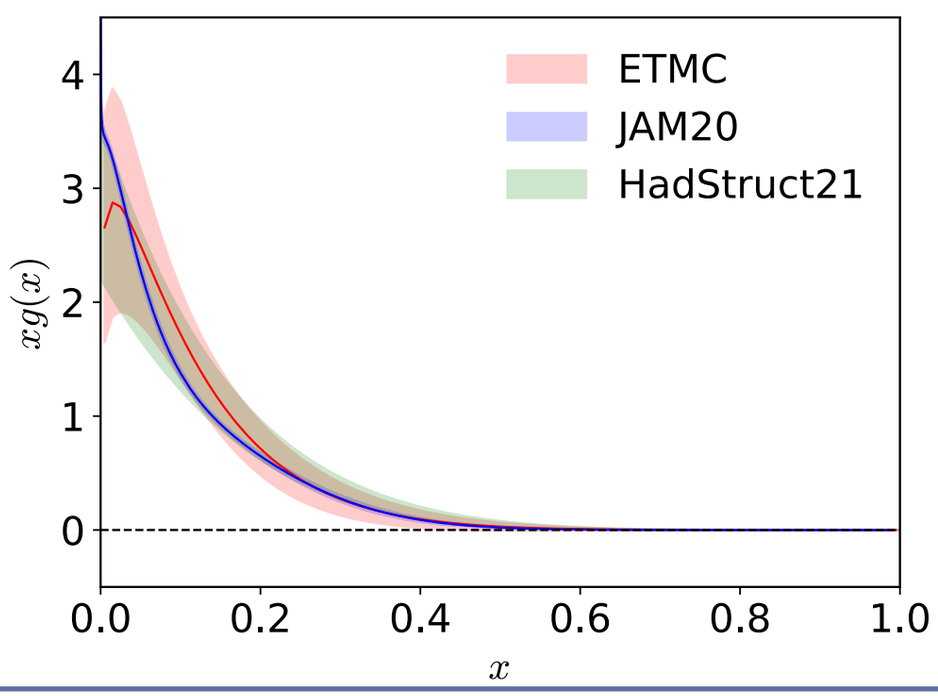
Gluon PDFs

Pion mass:	260 MeV
Lattice spacing:	0.093 fm
Volume:	$32^3 \times 64$

$\lvert\mathbf{P_3}\rvert$ $[\frac{2\pi}{L}]$	$\lvert\mathbf{P_3}\rvert$ [GeV]	N_{confs}	N_{src}	N_{dir}	Total statistics
0 to 4	0 - 1.67	1,134	200	6	1,360,800





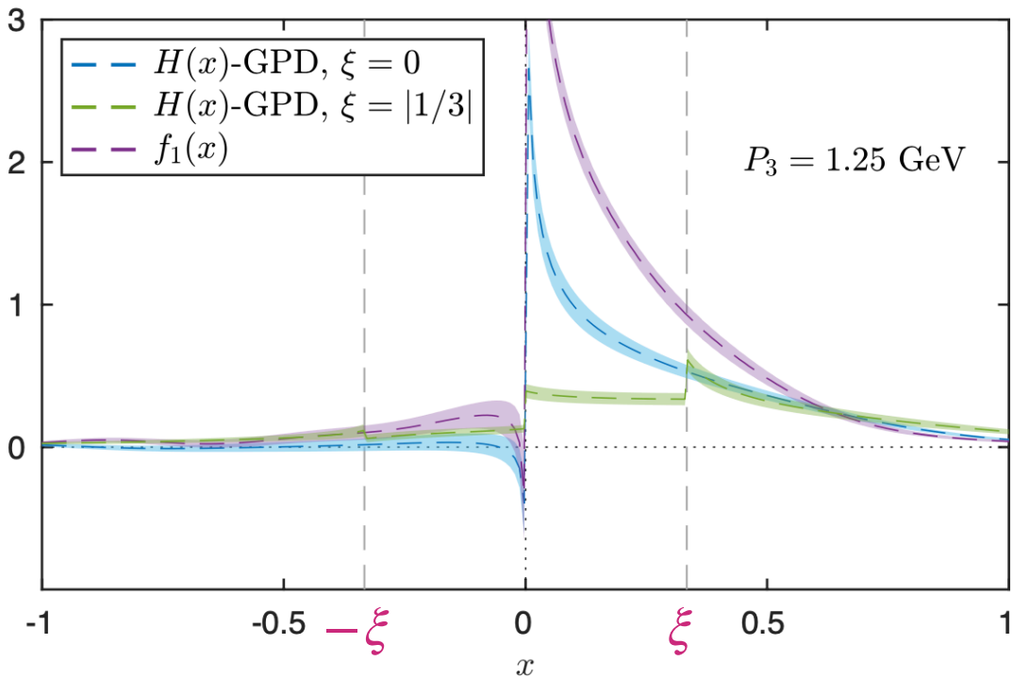


- ★ Controlling statistical noise is challenging
- ★ Large-v region unconstraint
- ★ Lattice results are promising

Isovector GPDs

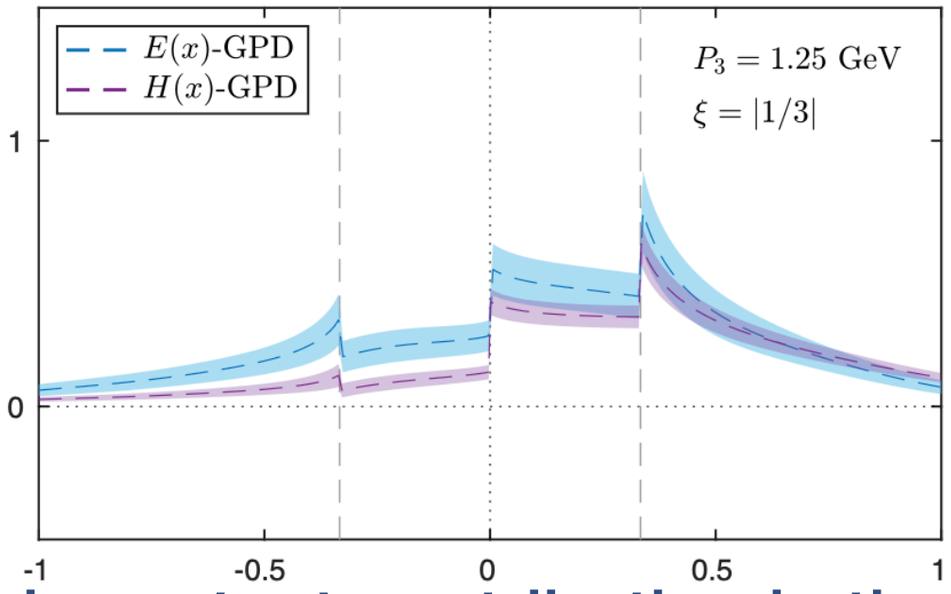
(status: qualitative understanding)

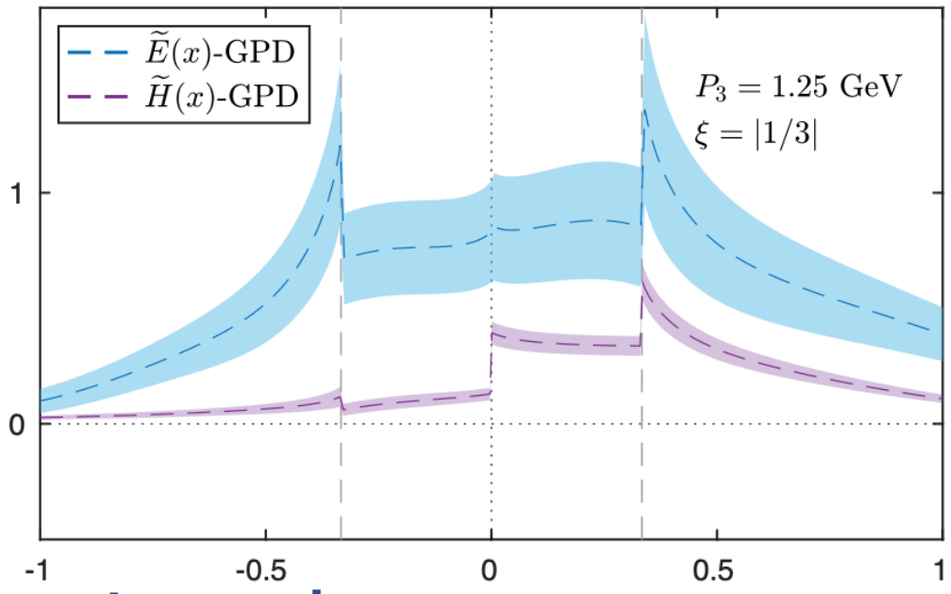
What can we currently do in lattice QCD?



[C. Alexandrou et al., PRL 125, 262001 (2020)]

- ★ ERBL/DGLAP: Qualitative differences
- ★ $\xi = \pm x$ inaccessible (formalism breaks down)
- ★ $x \to 1$ region: qualitatively comparison with power counting analysis [F. Yuan, PRD69 (2004) 051501, hep-ph/0311288]
  - ✦ t-dependence vanishes at large-x
  - ✦ $H(x,0)$ asymptotically equal to $f_1(x)$





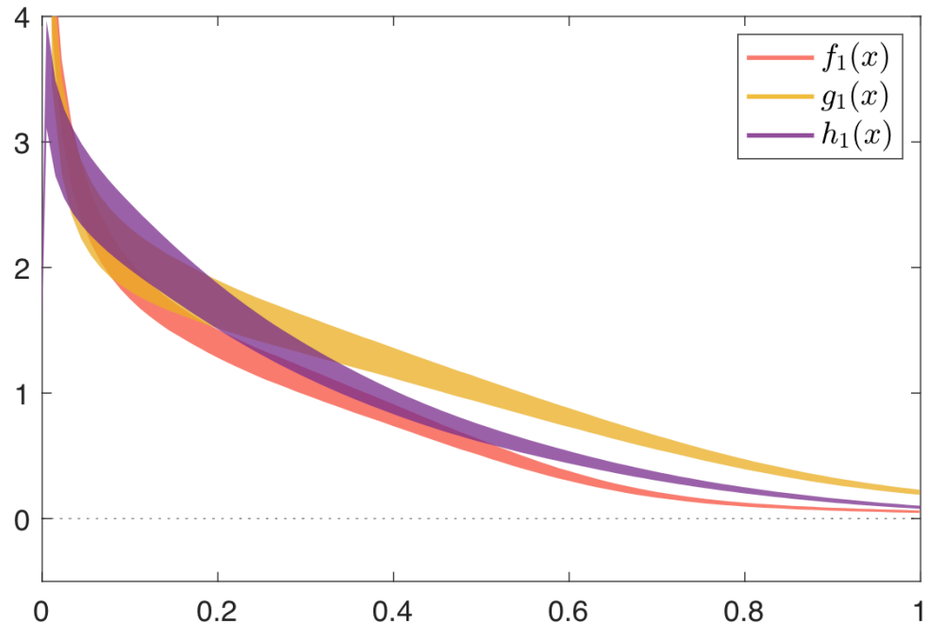
★ important contribution in the proton spin

$$\int_{-1}^{+1} dx x^2 H^q(x,\xi,t) = A_{20}^q(t) + 4\xi^2 C_{20}^q(t)\,, \qquad \int_{-1}^{+1} dx x^2 E^q(x,\xi,t) = B_{20}^q(t) - 4\xi^2 C_{20}^q(t)$$

What can we currently learn from lattice results?

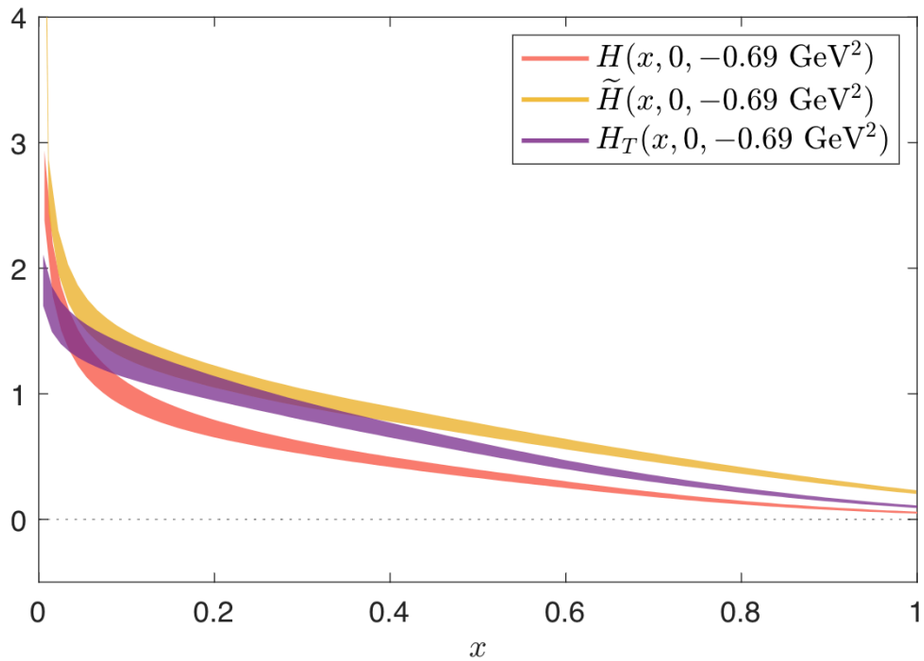
★ Qualitative understanding of GPDs and their relations

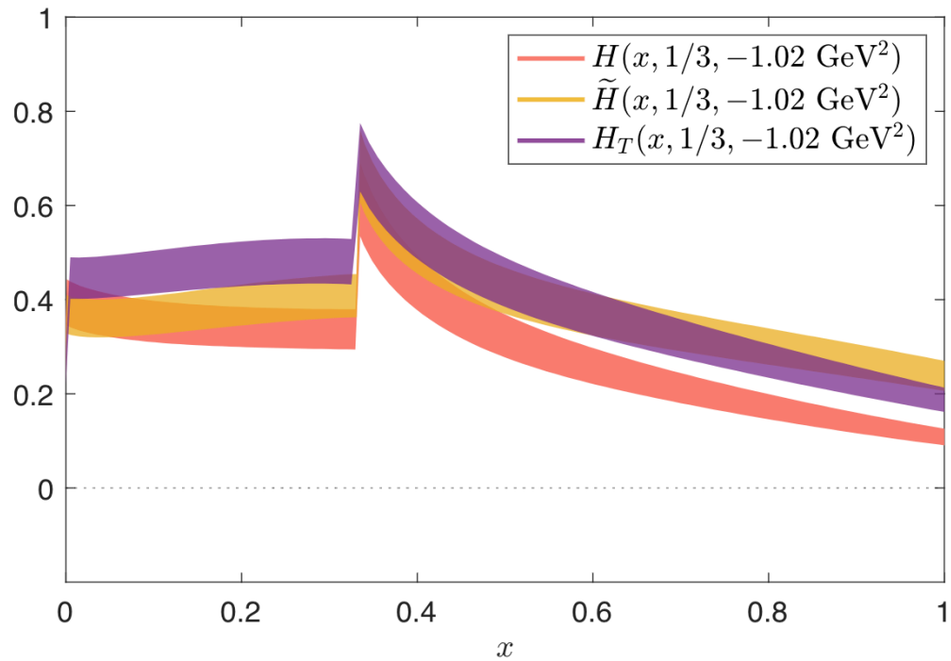
★ Qualitative understanding of ERBL and DGLAP regions



★ Relations can be identified for the t-dependence of GPDs

[C. Alexandrou et al., PRD 105, 034501 (2022)]





What can we currently check using lattice results?

★ Understanding of systematic effects through sum rules

★ Sum rules exist for quasi-GPDs

[S. Bhattacharya et al., PRD 102, 054021 (2020)]

$$\int_{-1}^{1} dx\, H_T(x,\xi,t) = \int_{-\infty}^{\infty} dx\, H_{Tq}(x,\xi,t,P_3) = A_{T10}(t)\,, \qquad \int_{-1}^{1} dx\, x\, H_T(x,\xi,t) = A_{T20}(t)\,,$$

$$\int_{-1}^{1} dx\, E_T(x,\xi,t) = \int_{-\infty}^{\infty} dx\, E_{Tq}(x,\xi,t,P_3) = B_{T10}(t)\,, \qquad \int_{-1}^{1} dx\, x\, E_T(x,\xi,t) = B_{T20}(t)\,,$$

$$\int_{-1}^{1} dx\, \widetilde{H}_T(x,\xi,t) = \int_{-\infty}^{\infty} dx\, \widetilde{H}_{Tq}(x,\xi,t,P_3) = \widetilde{A}_{T10}(t)\,, \qquad \int_{-1}^{1} dx\, x\, \widetilde{H}_T(x,\xi,t) = \widetilde{A}_{T20}(t)\,,$$

$$\int_{-1}^{1} dx\, \widetilde{E}_T(x,\xi,t) = \int_{-\infty}^{\infty} dx\, \widetilde{E}_{Tq}(x,\xi,t,P_3) = 0\,. \qquad \int_{-1}^{1} dx\, x\, \widetilde{E}_T(x,\xi,t) = 2\xi \widetilde{B}_{T21}(t)\,.$$

★ Lattice data on transversity GPDs

$$\int_{-2}^{2} dx H_{Tq}(x,0,-0.69\,\mathrm{GeV}^2,P_3)=\{0.65(4),\,0.64(6),\,0.81(10)\}\,, \qquad \int_{-2}^{2} dx H_{Tq}(x,\frac{1}{3},-1.02\,\mathrm{GeV}^2,1.25\,\mathrm{GeV})=0.49(5)\,,$$

$$\int_{-1}^{1} dx\, H_T(x,0,-0.69\,\mathrm{GeV}^2) = \{0.69(4),\,0.67(6),\,0.84(10)\}\,, \qquad \int_{-1}^{1} dx\, H_T(x,\frac{1}{3},-1.02\,\mathrm{GeV}^2) = 0.45(4)\,,$$

$$\int_{-1}^{1} dx\, x\, H_T(x,0,-0.69\,\mathrm{GeV}^2) = \{0.20(2),\,0.21(2),\,0.24(3)\}\,, \qquad \int_{-1}^{1} dx\, x\, H_T(x,\frac{1}{3},-1.02\,\mathrm{GeV}^2) = 0.15(2)\,.$$

$$A_{T10}(-0.69\,\mathrm{GeV}^2) = \{0.65(4)\,,0.65(6)\,,0.82(10)\}\,, \qquad A_{T10}(-1.02\,\mathrm{GeV}^2) = 0.49(5)$$

- lowest moments the same between quasi-GPDs and GPDs
- Values of moments decrease as t increases
- Higher moments suppressed compared to the lowest

twist-3 PDFs & GPDs

(status: exporation)

Why twist-3 GPDs?

$\mathcal{O}$ / Nucleon	γ^j	$\gamma^j \gamma^5$	σ^{jk}
U	G_1, G_2 G_3, G_4		
L		$\widetilde{G}_1, \widetilde{G}_2$ $\widetilde{G}_3, \widetilde{G}_4$	
T			$H_2'(x,\xi,t)$ $E_2'(x,\xi,t)$

Higher-twist distributions:

★ **Lack density interpretation, but can be sizable**

★ **Sensitive to soft dynamics**

★ **challenging to probe experimentally and isolate from leading-twist**

[Defurne et al., PRL 117, 26 (2016); Defurne et al., Nature Commun. 8, 1 (2017)]

★ **Needed for proton tomography**

★ **Related to certain spin-orbit correlations** [C. Lorce, PLB 735 (2014) 344, arXiv:1401.7784]

★ **Estimation on power corrections in hard exclusive processes (DVCS)**

★ $[\widetilde{H} + \widetilde{G}_2](x,\xi,t)$ **related to tomography of $F_\perp$ acting on the active q in DIS off a transversely polarized N right after the virtual photon absorbing**

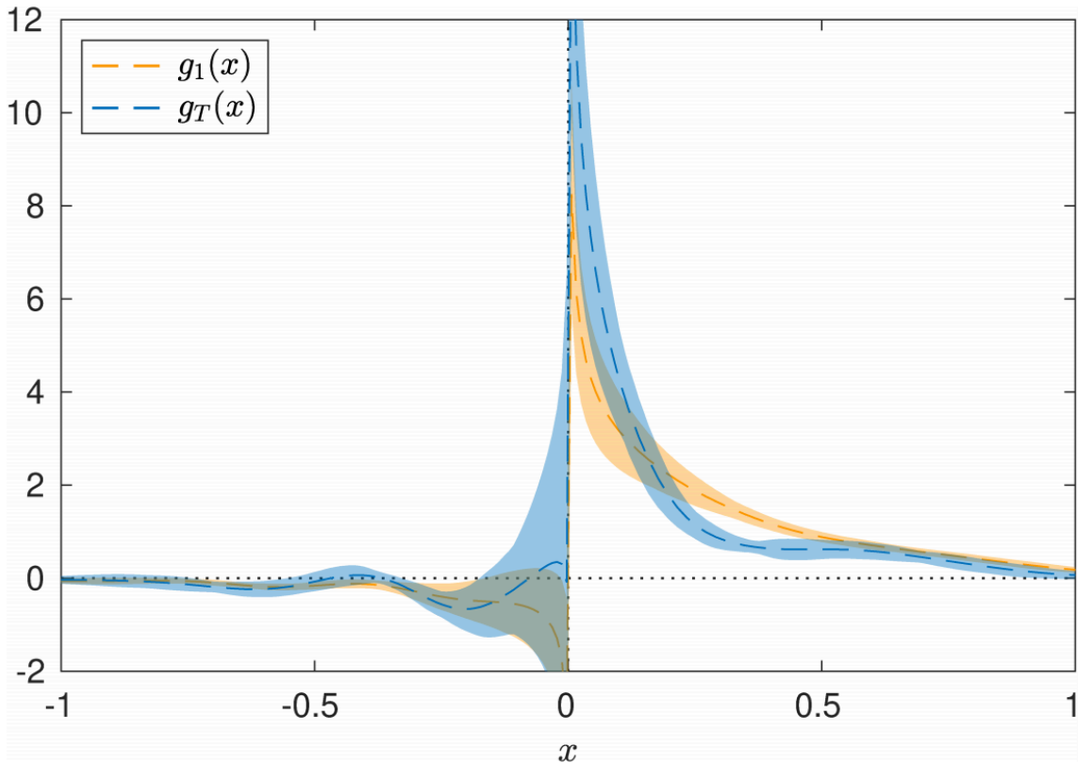
[M. Burkardt, PRD 88 (2013) 114502, arXiv:0810.3589]

★ $G_2(x,\xi,t)$ **related to** L_q **:**

$$L_q = -\int_{-1}^{1} dx\, x\, G_2^q(x,\xi,t=0)$$

[X. D. Ji, Phys. Rev. Lett. 78, 610 (1997), hep-ph/9603249], [M. Penttinen et al., PLB 491 (2000) 96, arXiv:hep-ph/0006321]

Twist-3 $g_T(x)$ PDF



[S. Bhattacharya et al., PRD 102 (2020) 11 (Editors Selection), arXiv:2004.04130]

Pion mass:	260 MeV
Lattice spacing:	0.093 fm
Volume:	32^3 x 64

Twist-3 counterpart as sizable as twist-2

Burkhardt-Cottingham sum rule important check

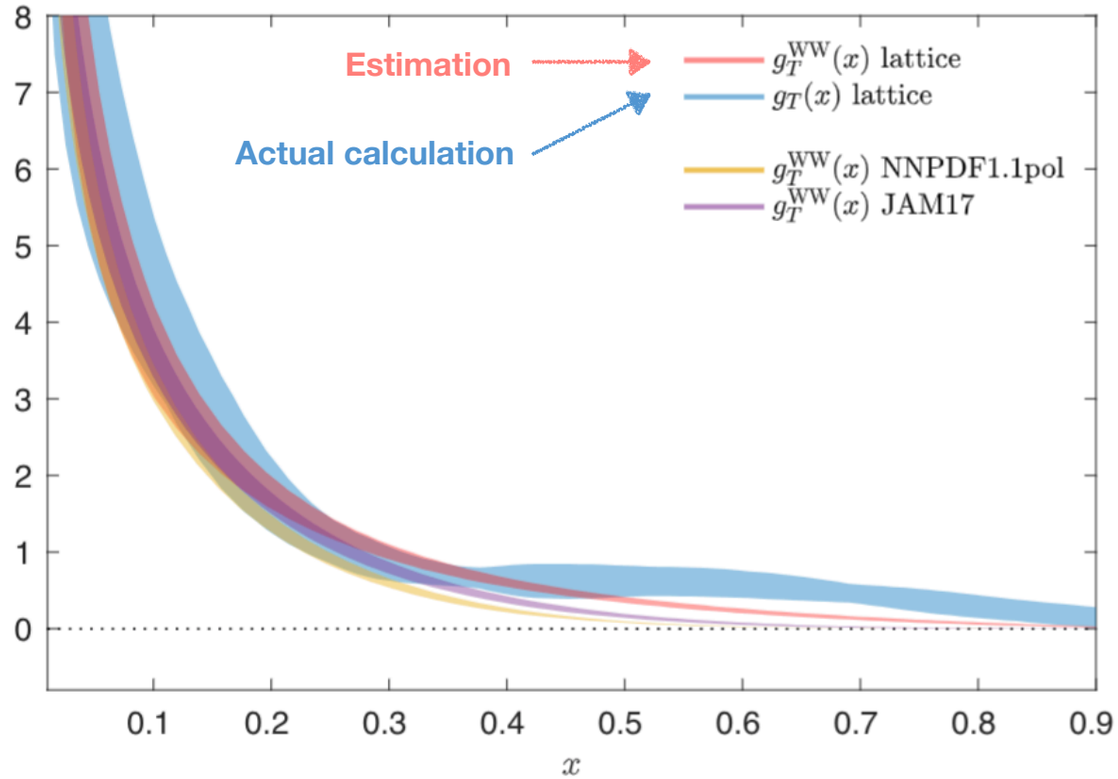
$$\int_{-1}^{1} dx\, g_1(x) - \int_{-1}^{1} dx\, g_T(x) = 0.01(20)$$

WW approximation: $g_T^{\mathrm{WW}}(x) = \int_x^1 \frac{dy}{y} g_1(y)$

twist-3 $g_T(x)$ determined by the twist-2 $g_1(x)$

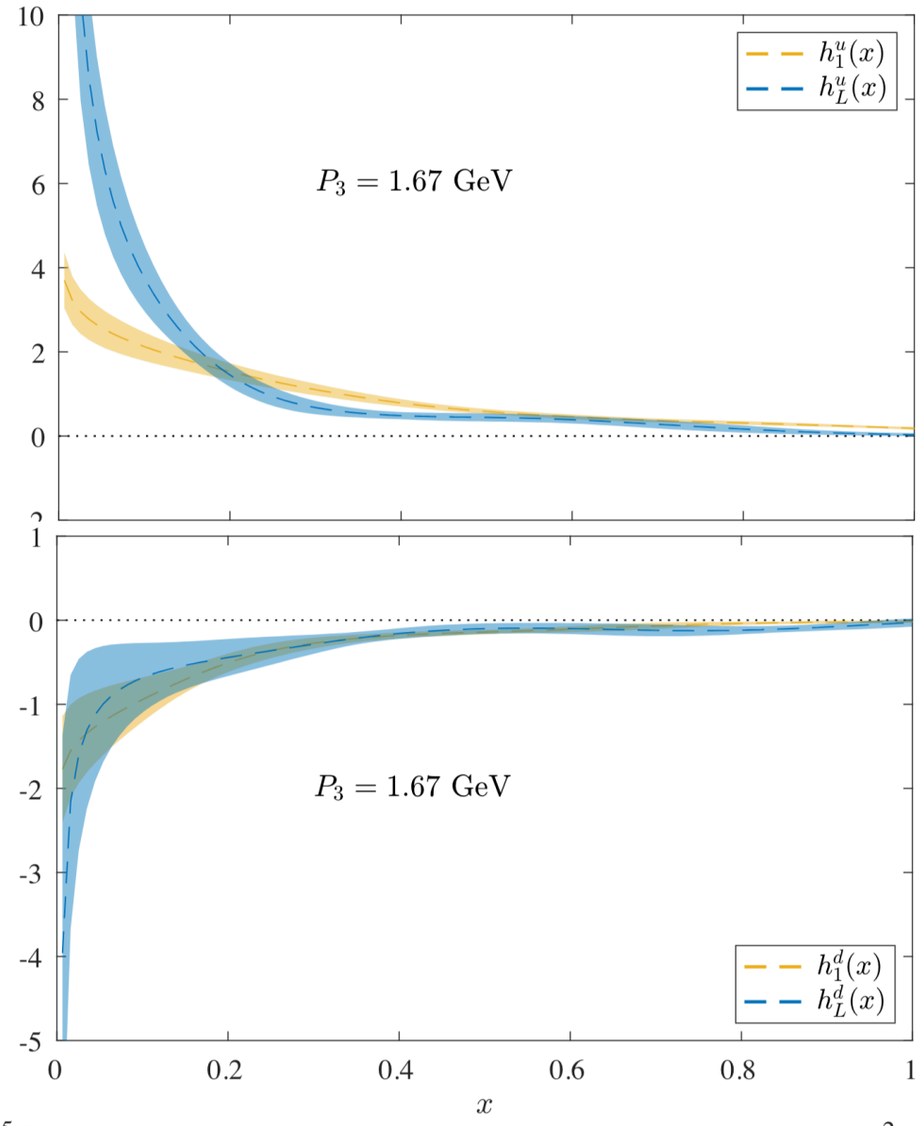
- $g_T(x)$ agrees with $g_T^{\mathrm{WW}}(x)$ for $x < 0.5$ (violations up to 30-40% possible)
- Violations of 15-40% expected from experimental data

[A. Accardi et al., JHEP 11 (2009) 093]



Twist-3 $h_L(x)$ PDF

Pion mass:	260 MeV
Lattice spacing:	0.093 fm
Volume:	32^3 x 64



- up-quark dominant in particular for x<0.5
- Large-x: $h^u_{1,L} \sim 2h^d_{1,L}$

Burkhardt-Cottingham valid for quasi-$h_L(x)$

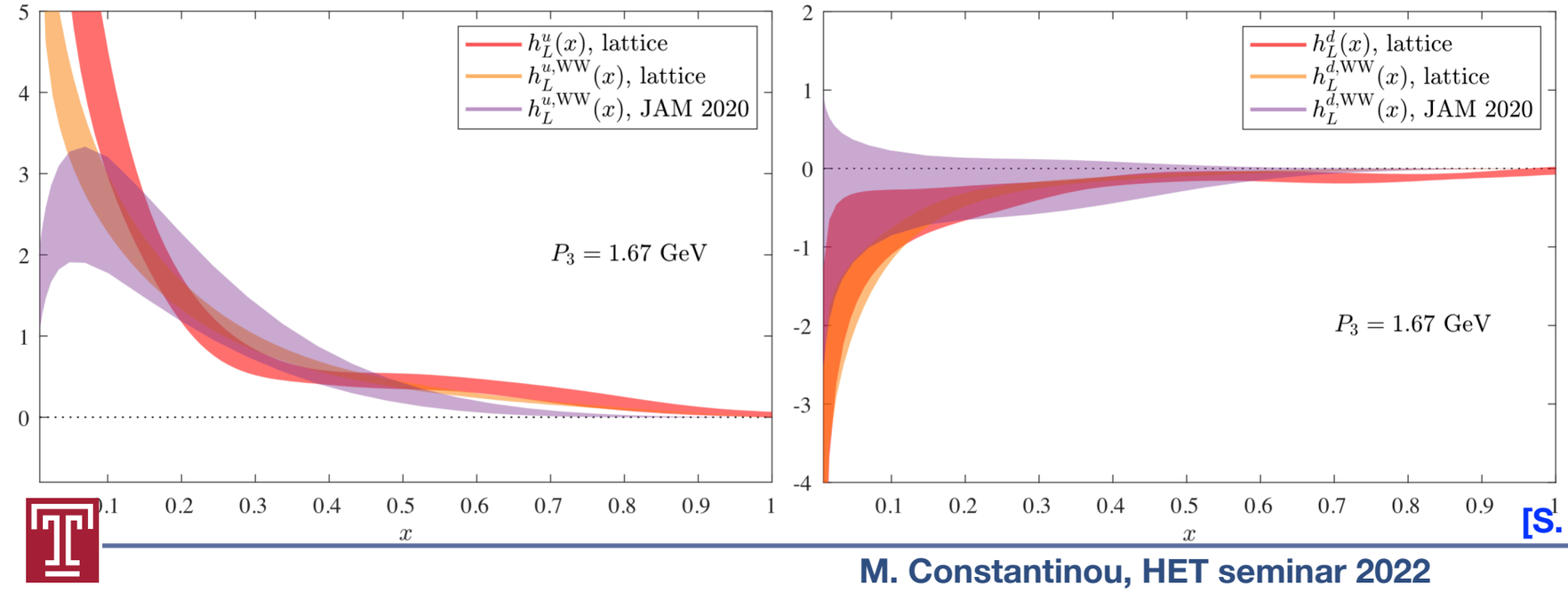
[S. Bhattacharya, A. Metz, arXiv:2105.07282]

$$\int_{-1}^{1} dx\, \tilde{h}_L(x, P_3) = \int_{-1}^{1} dx\, \tilde{h}_1(x, P_3) = g_T$$

$$\int dx\, \tilde{h}_L(x, 0.83\,\text{GeV}) = 1.13(08)\,, \qquad \int dx\, \tilde{h}_1(x, 0.83\,\text{GeV}) = 1.02(07)$$

$$\int dx\, \tilde{h}_L(x, 1.25\,\text{GeV}) = 1.09(10)\,, \qquad \int dx\, \tilde{h}_1(x, 1.25\,\text{GeV}) = 1.07(08)$$

$$\int dx\, \tilde{h}_L(x, 1.67\,\text{GeV}) = 1.03(16)\,, \qquad \int dx\, \tilde{h}_1(x, 1.67\,\text{GeV}) = 0.94(10)$$



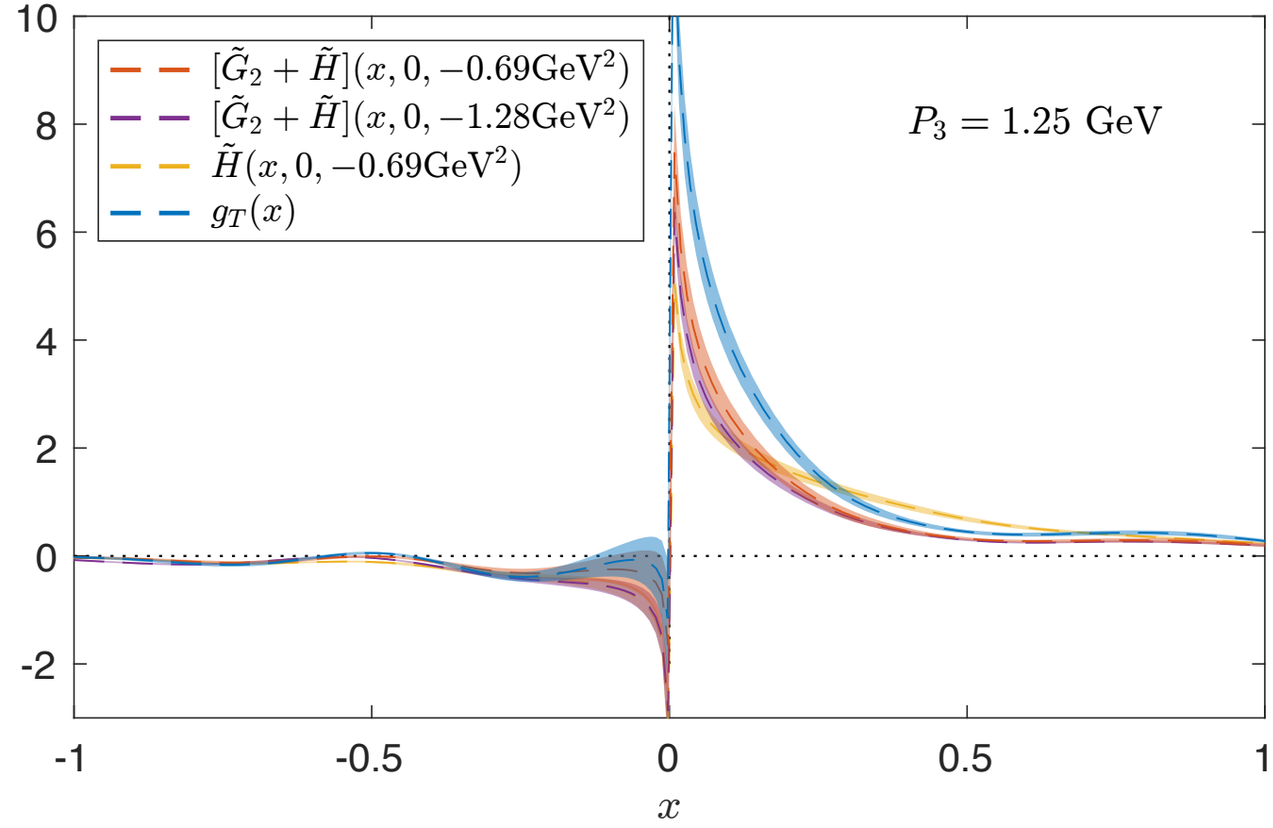
- h_L^u dominant - tension between h_L & h_L^{WW}
- h_L^d <0 and decays faster then h_L^u

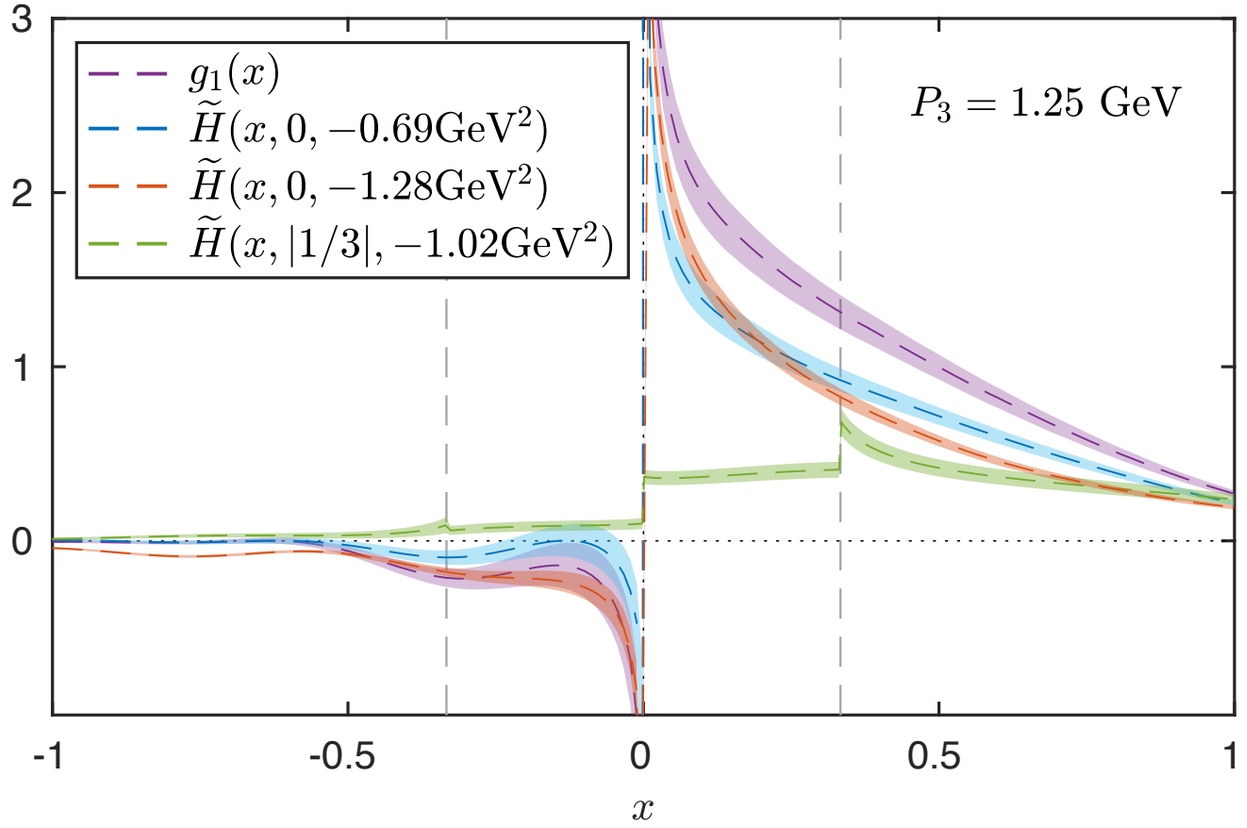
[S. Bhattacharya et al., arXiv:2107.02574]

Twist-3 GPDs

★ Twist-3 GPDs

PRELIMINARY



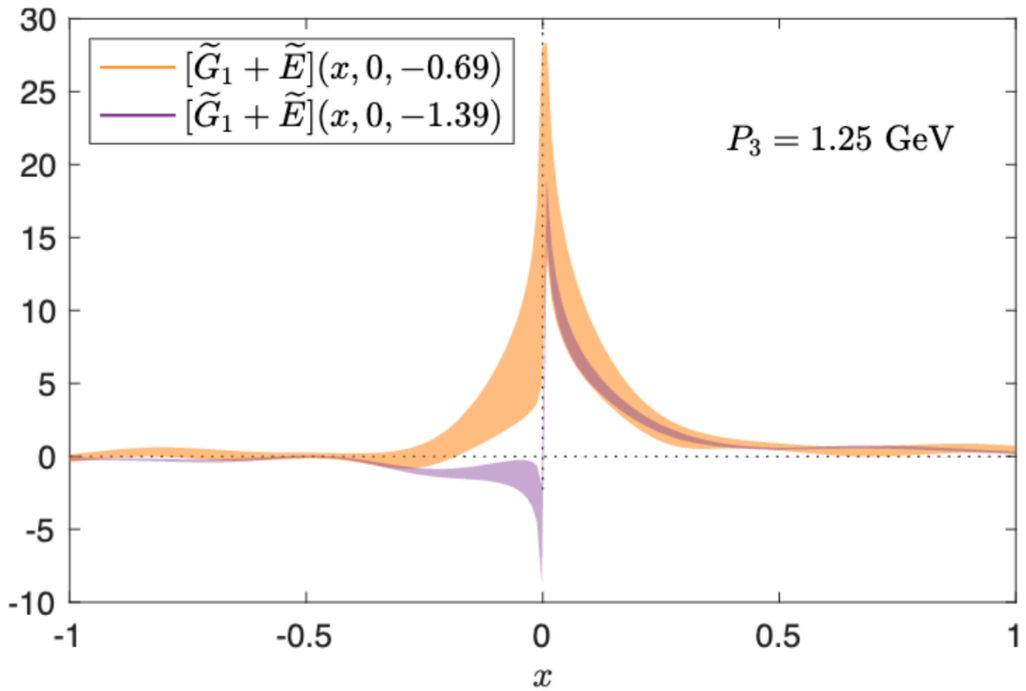


[S. Bhattacharya et al., PoS LATTICE2021 (2022) 054 arXiv:2112.05538]

★ $g_T(x)$: dominant distribution

★ $\widetilde{H} + \widetilde{G}_2$ similar in magnitude to $\widetilde{H}$

★ $\widetilde{G}_2$ is expected to be small



GPDs in alternative frames

(status: innovative)

Definition of GPDs in Euclidean lattice

★ Calculation expected to be performed in symmetric frame to extract the “standard” GPDs

★ Symmetric frame requires separate calculations at each t

Let’s rethink calculation of GPDs !

1st goal:

Extraction of GPDs in the symmetric frame using lattice correlators calculated in non-symmetric frames

2nd goal:

New definition of Lorentz covariant quasi-GPDs that may have faster convergence to light-cone GPDs (elimination of kinematic corrections)

Theoretical setup

[S. Bhattacharya et al., arXiv:2209.05373]

★ Parametrization of matrix elements in Lorentz invariant amplitudes

$$F^{\mu}_{\lambda,\lambda'} = \bar{u}(p',\lambda')\left[\frac{P^{\mu}}{M}A_1 + z^{\mu}MA_2 + \frac{\Delta^{\mu}}{M}A_3 + i\sigma^{\mu z}MA_4 + \frac{i\sigma^{\mu\Delta}}{M}A_5 + \frac{P^{\mu}i\sigma^{z\Delta}}{M}A_6 + \frac{z^{\mu}i\sigma^{z\Delta}}{M}A_7 + \frac{\Delta^{\mu}i\sigma^{z\Delta}}{M}A_8\right]u(p,\lambda)$$

Advantages

- Applicable to any kinematic frame and have definite symmetries
- Lorentz invariant amplitudes A_i can be related to the standard H, E GPDs
- Quasi H, E may be redefined (Lorentz covariant) to eliminate $1/P_3$ contributions:

$$H(z\cdot P, z\cdot\Delta, t=\Delta^2, z^2) = A_1 + \frac{\Delta_{s/a}\cdot z}{P_{avg,s/a}\cdot z}A_3$$

$$E(z\cdot P, z\cdot\Delta, t=\Delta^2, z^2) = -A_1 - \frac{\Delta_{s/a}\cdot z}{P_{avg,s/a}\cdot z}A_3 + 2A_5 + 2P_{avg,s/a}\cdot zA_6 + 2\Delta_{s/a}\cdot zA_8$$

★ Proof-of-concept calculation (zero quasi-skewness):

- symmetric frame: $\vec{p}^{\,s}_f = \vec{P} + \frac{\vec{Q}}{2}$, $\vec{p}^{\,s}_i = \vec{P} - \frac{\vec{Q}}{2}$, $t^s = -\vec{Q}^2$

- asymmetric frame: $\vec{p}^{\,a}_f = \vec{P}$, $\vec{p}^{\,a}_i = \vec{P} - \vec{Q}$, $t^a = -\vec{Q}^2 + (E_f - E_i)^2$

Matrix element decomposition

Symmetric

$$C_s = \frac{2m^2}{E(E+m)}$$

$$\Gamma_0 = \frac{1}{2}(1+\gamma^0)$$

$$\Gamma_j = \frac{i}{4}(1+\gamma^0)\gamma^5\gamma^j \quad (j = 1,2,3)$$

$$\Pi_s^0(\Gamma_0) = C_s \left(\frac{E\left(E(E+m) - P_3^2\right)}{2m^3} A_1 + \frac{(E+m)\left(-E^2+m^2+P_3^2\right)}{m^3} A_5 + \frac{EP_3\left(-E^2+m^2+P_3^2\right)z}{m^3} A_6 \right)$$

$$\Pi_s^0(\Gamma_1) = i\, C_s \left(\frac{EP_3Q_2}{4m^3} A_1 - \frac{(E+m)P_3Q_2}{2m^3} A_5 - \frac{E\left(P_3^2+m(E+m)\right)zQ_2}{2m^3} A_6 \right)$$

$$\Pi_s^0(\Gamma_2) = i\, C_s \left(-\frac{EP_3Q_1}{4m^3} A_1 + \frac{(E+m)P_3Q_1}{2m^3} A_5 + \frac{E\left(P_3^2+m(E+m)\right)zQ_1}{2m^3} A_6 \right)$$

Novel feature: z-dependence

Asymmetric

$$C_a = \frac{2m^2}{\sqrt{E_iE_f(E_i+m)(E_f+m)}}$$

$$\Pi_0^a(\Gamma_0) = C_a \left(-\frac{(E_f+E_i)(E_f-E_i-2m)(E_f+m)}{8m^3} A_1 - \frac{(E_f-E_i-2m)(E_f+m)(E_f-E_i)}{4m^3} A_3 \right.$$
$$+\frac{(E_i-E_f)P_3z}{4m} A_4 + \frac{(E_f+E_i)(E_f+m)(E_f-E_i)}{4m^3} A_5 + \frac{E_f(E_f+E_i)P_3(E_f-E_i)z}{4m^3} A_6$$
$$\left. +\frac{E_fP_3(E_f-E_i)^2z}{2m^3} A_8 \right)$$

$$\Pi_0^a(\Gamma_1) = i\, C_a \left(\frac{(E_f+E_i)P_3Q_2}{8m^3} A_1 + \frac{(E_f-E_i)P_3Q_2}{4m^3} A_3 + \frac{(E_f+m)Q_2z}{4m} A_4 - \frac{(E_f+E_i+2m)P_3Q_2}{4m^3} A_5 \right.$$
$$\left. -\frac{E_f(E_f+E_i)(E_f+m)Q_2z}{4m^3} A_6 - \frac{E_f(E_f-E_i)(E_f+m)Q_2z}{2m^3} A_8 \right)$$

No definite symmetries for Π_μ^a

$$\Pi_0^a(\Gamma_2) = i\, C_a \left(-\frac{(E_f+E_i)P_3Q_1}{8m^3} A_1 - \frac{(E_f-E_i)P_3Q_1}{4m^3} A_3 - \frac{(E_f+m)Q_1z}{4m} A_4 + \frac{(E_f+E_i+2m)P_3Q_1}{4m^3} A_5 \right.$$
$$\left. +\frac{E_f(E_f+E_i)(E_f+m)Q_1z}{4m^3} A_6 + \frac{E_f(E_f-E_i)(E_f+m)Q_1z}{2m^3} A_8 \right)$$

Lorentz-Invariant amplitudes

Symmetric

$$A_1 = \frac{\left(m(E+m)+P_3^2\right)}{E(E+m)}\Pi_0^s(\Gamma_0) - i\,\frac{P_3 Q_1}{2E(E+m)}\Pi_0^s(\Gamma_2) - \frac{Q_1}{2E}\Pi_2^s(\Gamma_3)$$

$$A_5 = -\frac{E}{Q_1}\Pi_2^s(\Gamma_3)$$

$$A_6 = \frac{P_3}{2Ez(E+m)}\Pi_0^s(\Gamma_0) + i\,\frac{\left(P_3^2 - E(E+m)\right)}{EQ_1 z(E+m)}\Pi_0^s(\Gamma_2) + \frac{P_3}{EQ_1 z}\Pi_2^s(\Gamma_3)$$

$$A_1 = \frac{2m^2}{E_f(E_i+m)}\frac{\Pi_0^a(\Gamma_0)}{C_a} + i\,\frac{2(E_f-E_i)P_3m^2}{E_f(E_f+m)(E_i+m)Q_1}\frac{\Pi_0^a(\Gamma_2)}{C_a} + \frac{2(E_i-E_f)P_3m^2}{E_f(E_f+E_i)(E_f+m)(E_i+m)}\frac{\Pi_1^a(\Gamma_2)}{C_a}$$
$$+i\,\frac{2(E_i-E_f)m^2}{E_f(E_i+m)Q_1}\frac{\Pi_1^a(\Gamma_0)}{C_a} + \frac{2(E_i-E_f)P_3m^2}{E_f(E_f+E_i)(E_f+m)(E_i+m)}\frac{\Pi_2^a(\Gamma_1)}{C_a} + \frac{2(E_f-E_i)m^2}{E_f(E_i+m)Q_1}\frac{\Pi_2^a(\Gamma_3)}{C_a}$$

$$A_5 = \frac{m^2P_3}{E_f(E_f+m)(E_i+m)}\frac{\Pi_2^a(\Gamma_1)}{C_a} - \frac{(E_f+E_i)m^2}{E_f(E_i+m)Q_1}\frac{\Pi_2^a(\Gamma_3)}{C_a}$$

$$A_6 = \frac{P_3m^2}{E_f^2(E_f+m)(E_i+m)z}\frac{\Pi_0^a(\Gamma_0)}{C_a} + i\,\frac{(E_f-E_i-2m)m^2}{E_f^2(E_i+m)Q_1z}\frac{\Pi_0^a(\Gamma_2)}{C_a} + i\,\frac{(E_i-E_f)P_3m^2}{E_f^2(E_f+m)(E_i+m)Q_1z}\frac{\Pi_1^a(\Gamma_0)}{C_a}$$
$$+\frac{(-E_f+E_i+2m)m^2}{E_f^2(E_f+E_i)(E_i+m)z}\frac{\Pi_1^a(\Gamma_2)}{C_a} + \frac{2(m-E_f)m^2}{E_f^2(E_f+E_i)(E_i+m)z}\frac{\Pi_2^a(\Gamma_1)}{C_a} + \frac{2P_3m^2}{E_f^2(E_i+m)Q_1z}\frac{\Pi_2^a(\Gamma_3)}{C_a}$$

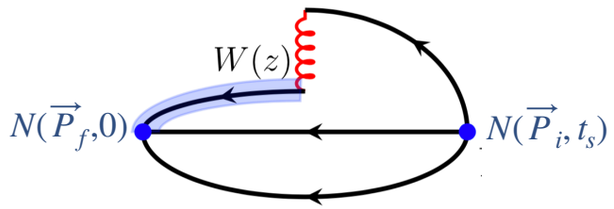
- ★ Asymmetric frame equations more complex
- ★ A_i have definite symmetries
- ★ System of 8 independent matrix elements to disentangle the A_i

Parameters of calculation

★ Nf=2+1+1 twisted mass (TM) fermions & clover improvement

Pion mass:	260 MeV
Lattice spacing:	0.093 fm
Volume:	32^3 x 64
Spatial extent:	3 fm

★ Calculation:
- isovector combination
- zero skewness
- T_{sink}=1 fm



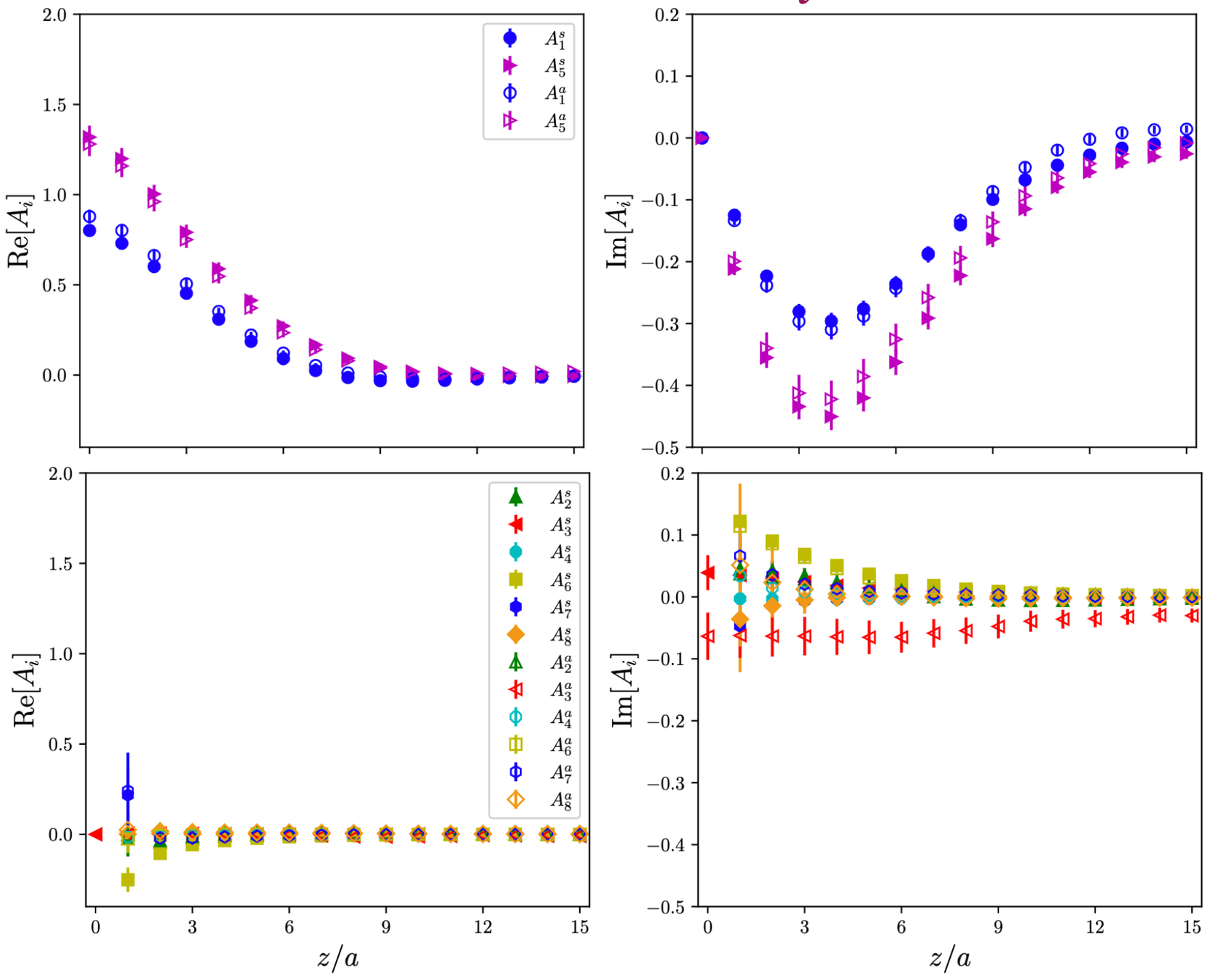
frame	P_3 [GeV]	$\mathbf{Q}$ $[\frac{2\pi}{L}]$	$-t$ [GeV^2]	ξ	$N_{\rm ME}$	$N_{\rm confs}$	$N_{\rm src}$	$N_{\rm tot}$
symm	1.25	(±2,0,0), (0,±2,0)	0.69	0	8	249	8	15936
non-symm	1.25	(±2,0,0), (0,±2,0)	0.64	0	8	269	8	17216

Small difference: $t^s = -\vec{Q}^2$ $t^a = -\vec{Q}^2 + (E_f - E_i)^2$

$A(-0.64\text{GeV}^2) \sim A(-0.69\text{GeV}^2)$

★ Computational cost:
- symmetric frame 4 times more expensive than asymmetric frame for same set of $\vec{Q}$ (requires separate calculations at each t)

Results: A_i



- ★ A_1, A_5 dominant contributions
- ★ Full agreement in two frames for both Re and Im parts of A_1, A_5
- ★ Remaining A_i suppressed (at least for this kinematic setup and $\xi = 0$)

Π_H, Π_E in terms of A_i

★ Mapping of $\{\Pi_H, \Pi_E\}$ to A_i using $F^{[\gamma^0]} \sim \left[\gamma^0 H_{\mathrm{Q}(0)}(x,\xi,t;P^3) + \frac{i\sigma^{0\mu}\Delta_\mu}{2M} E_{\mathrm{Q}(0)}(x,\xi,t;P^3)\right]$ in each frame leading to frame dependent relations:

$(\xi = 0)$

$$\Pi_H^s = A_1 + \frac{zQ_1^2}{2P_3} A_6$$

$$\Pi_E^s = -A_1 - \frac{m^2 z}{P_3} A_4 + 2A_5 - \frac{z\left(4E^2 + Qx^2 + Qy^2\right)}{2P_3} A_6$$

1st approach: extraction of $\{\Pi_H^s, \Pi_E^s\}$ using A_i from any frame (universal)

$$\Pi_H^a = A_1 + \frac{Q_0}{P_0} A_3 + \frac{m^2 z Q_0}{2P_0 P_3} A_4 + \frac{z(Q_0^2 + Q_\perp^2)}{2P_3} A_6 + \frac{z(Q_0^3 + Q_0 Q_\perp^2)}{2P_0 P_3} A_8$$

$$\Pi_E^a = -A_1 - \frac{Q_0}{P_0} A_3 - \frac{m^2 z(Q_0 + 2P_0)}{2P_0 P_3} A_4 + 2A_5 - \frac{z\left(Q_0^2 + 2P_0 Q_0 + 4P_0^2 + Q_\perp^2\right)}{2P_3} A_6 - \frac{zQ_0\left(Q_0^2 + 2Q_0 P_0 + 4P_0^2 + Q_\perp^2\right)}{2P_0 P_3} A_8$$

2nd approach: extraction of $\{\Pi_H, \Pi_E\}$ from a purely asymmetric frame; GPDs differ in functional form from $\{\Pi_H^s, \Pi_E^s\}$

★ Definition of Lorentz invariant Π_H & Π_E

$(\xi = 0)$

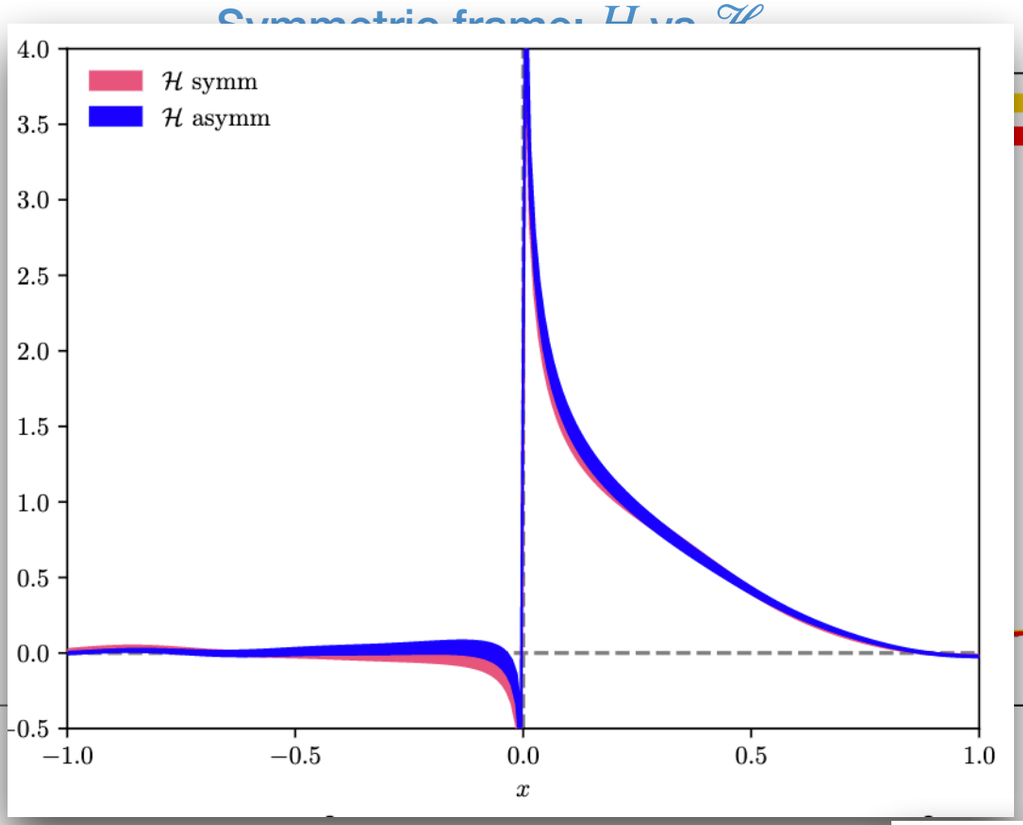
$$\Pi_H^{\mathrm{impr}} = A_1$$

$$\Pi_E^{\mathrm{impr}} = -A_1 + 2A_5 + 2zP_3 A_6$$

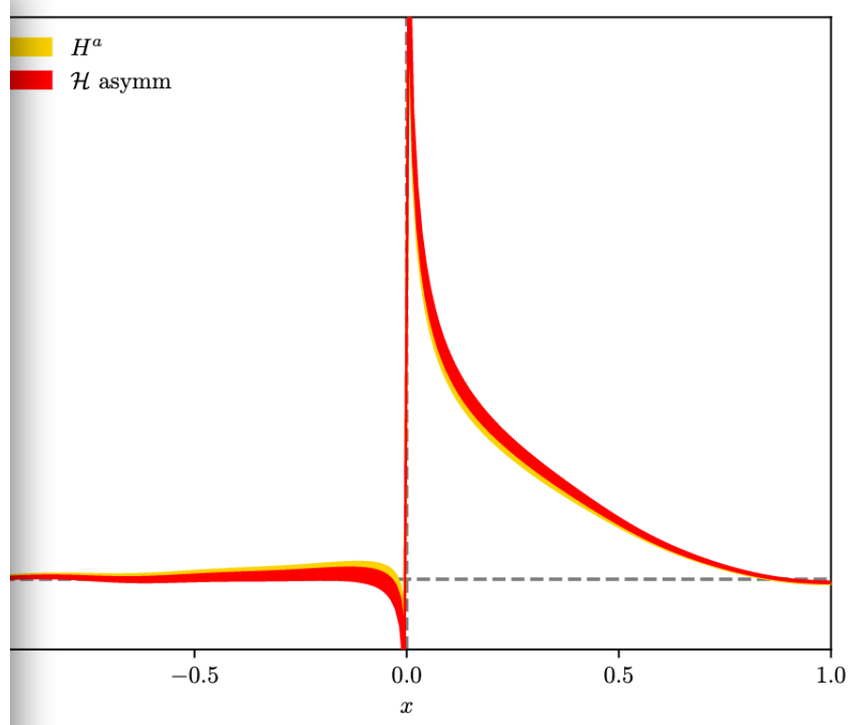
3rd approach: use redefined Lorentz covariant $\{\Pi_H, \Pi_E\}$ in desired frame

Results: H – GPD

Symmetric frame: H vs $\mathscr{H}$

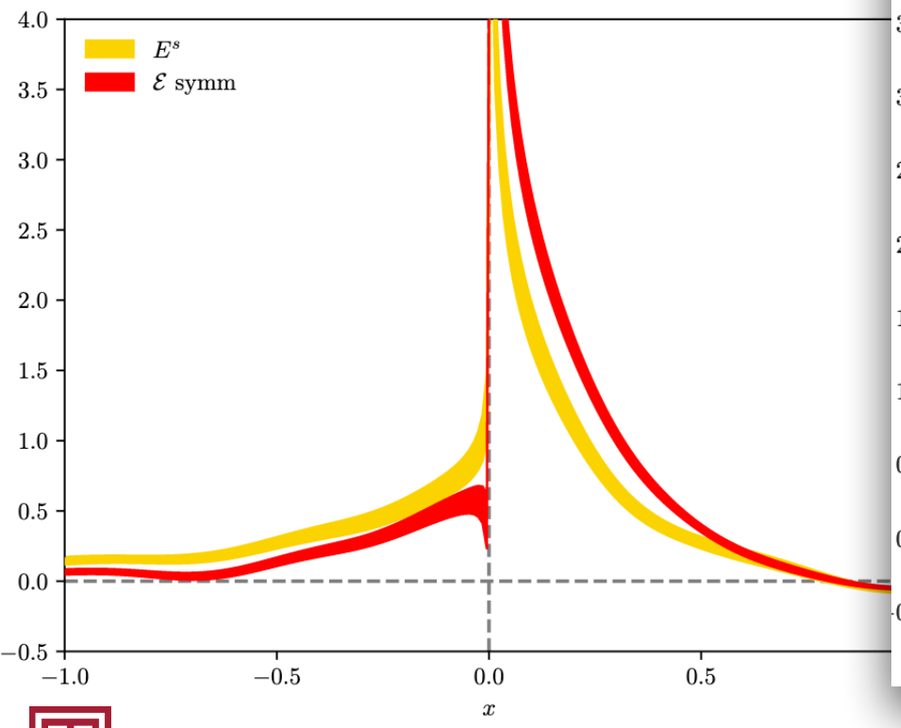


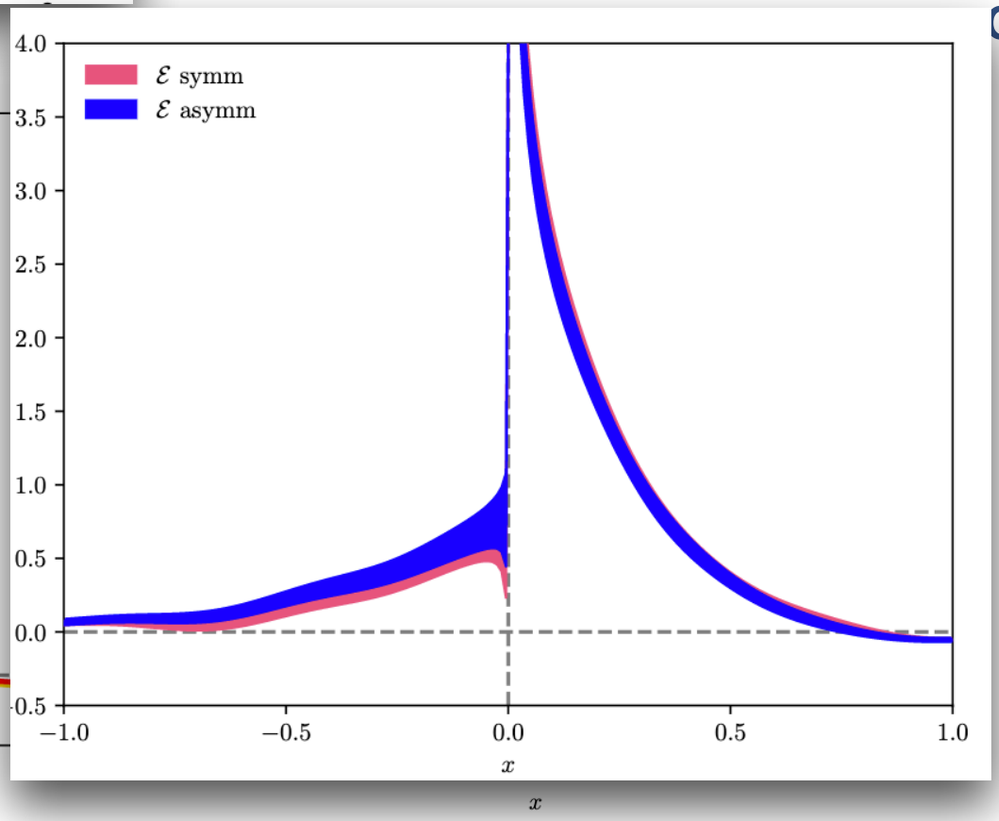
Asymmetric frame: H vs $\mathscr{H}$



Similar results for H and $\mathscr{H}$ for both frames (agreement not by construction)

Symmetric frame: E vs $\mathscr{E}$



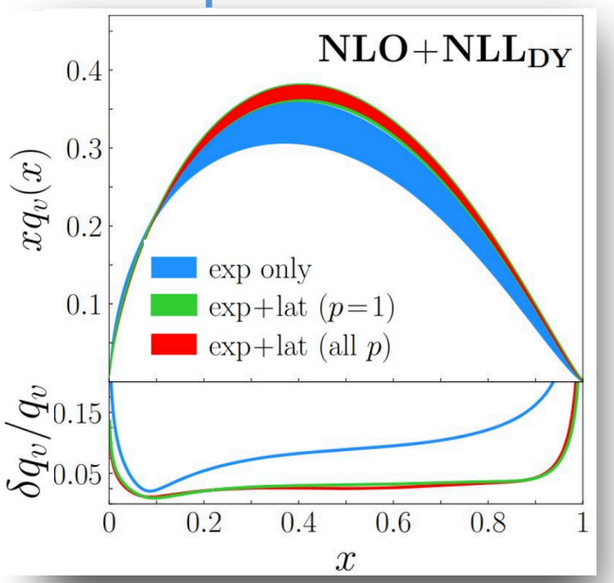


Differences between E and $\mathscr{E}$ for both frames (agreement not by construction)

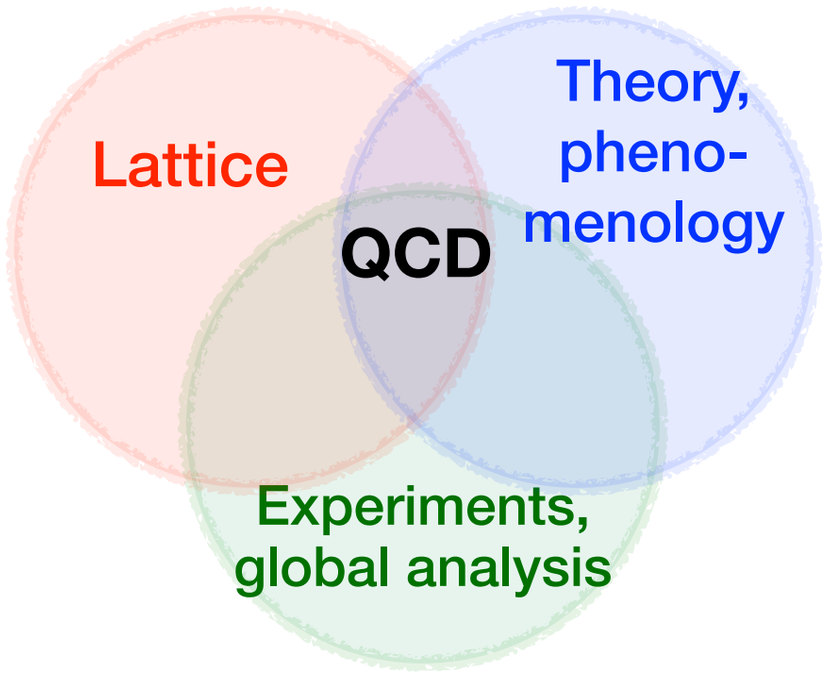
Agreement between frames for $\mathscr{H}$ and $\mathscr{E}$ (agreement by construction)

Synergies: constraints & predictive power of lattice QCD

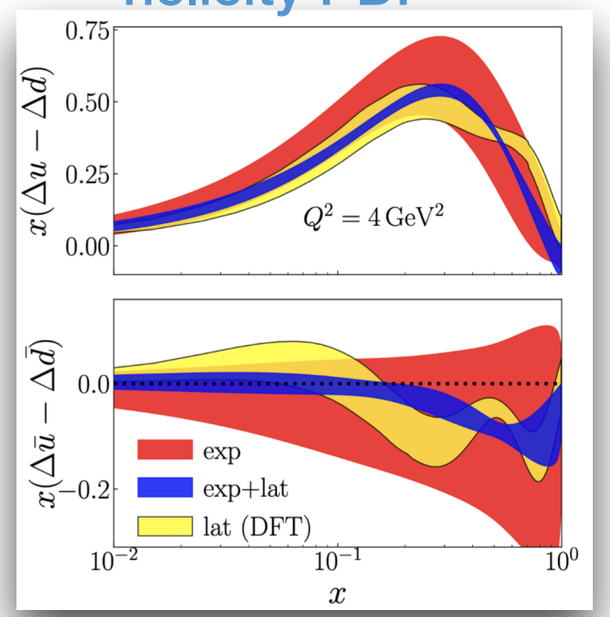
pion PDF



[JAM/HadStruc, PRD105 (2022) 114051]

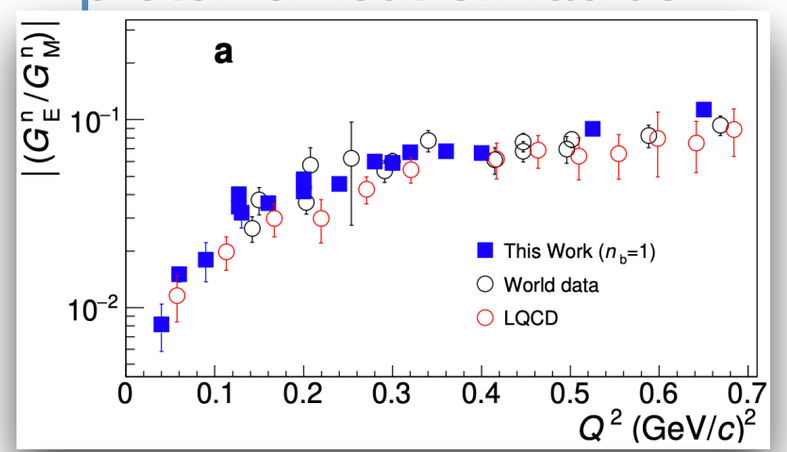


helicity PDF



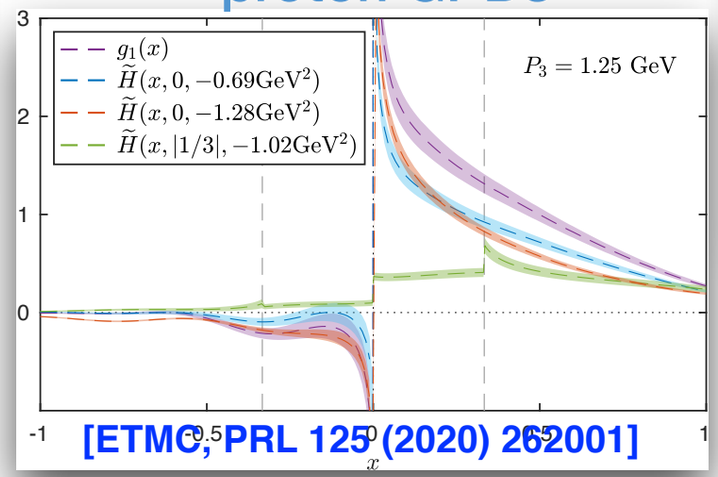
[JAM & ETMC, PRD 103 (2021) 016003]

proton & neutron radius



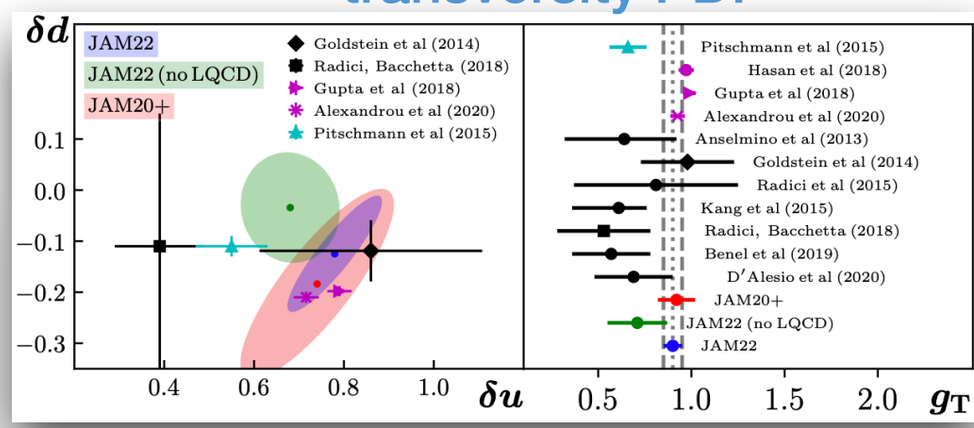
[Atac et al., Nature Comm. 12, 1759 (2021)]

proton GPDs



[ETMC, PRL 125 (2020) 262001]

transversity PDF



[JAM, PRD 106 (2022) 3, 034014]

Summary

- ★ Tomographic imaging of proton has central role in the science program of JLab
- ★ Lattice QCD data on GPDs will play an important role in the pre-EIC era and can complement experimental efforts of JLab@12GeV
- ★ New proposal for Lorentz invariant decomposition has great advantages:
  - significant reduction of computational cost
  - access to a broad range of t and ξ
- ★ Future calculations have the potential to transform the field of GPDs
- ★ Synergy with phenomenology is an exciting prospect!

U.S. DEPARTMENT OF ENERGY INCITE LEADERSHIP COMPUTING

Thank you

U.S. DEPARTMENT OF ENERGY | Office of Science

DOE Early Career Award (NP)
Grant No. DE-SC0020405